PERFORMANCE AMPLIFICATION OF PV SYSTEM CONFIGURATIONS UNDER PARTIAL SHADING CONDITIONS EMPLOYING MAGIC SQUARE TECHNIQUE

A Thesis Submitted

IN PARTIAL FULFILLMENT OF THE REQUIREMENTS

FOR THE DEGREE OF

DOCTOR OF PHILOSOPHY

IN

Electrical Engineering

Department of Electrical, Electronics and Communication Engineering

By

SNIGDHA SHARMA

Regd. No. – 18SECE3010002

Under the Supervision of

Dr. Lokesh Varshney

UTTAR PRADESH

[2022]

STATEMENT OF THESIS PREPARATION

---

1. Thesis title: Performance Amplification of PV System Configurations Under Partial Shading Conditions Employing Magic Square Technique.

2. Degree for which the thesis is submitted: Doctor of Philosophy in Electrical Engineering, Department of Electrical, Electronics and Communication Engineering.

3. Thesis Guide was referred to for preparing the thesis.

4. Specifications regarding thesis format have been closely followed.

5. The contents of the thesis have been organized based on the guidelines.

6. The thesis has been prepared without resorting to plagiarism.

7. All sources used have been cited appropriately.

8. The thesis has not been submitted elsewhere for a degree.

(Signature of the Student)
Name: Snigdha Sharma
Roll No: 18SECE3010002

APPROVAL SHEET

This thesis entitled "Performance Amplification of PV System Configurations Under Partial Shading Conditions Employing Magic Square Technique" by Ms. Snigdha Sharma is approved for the degree of Doctor of Philosophy.

Examiners

Supervisor (s)

Chairman

Date: ----------
Place: ----------

CANDIDATE'S DECLARATION

I hereby certify that the work which is being presented in the thesis, entitled "**Performance Amplification of PV System Configurations Under Partial Shading Conditions Employing Magic Square Technique**" in fulfillment of the requirements for the award of the degree of Doctor of Philosophy in Faculty and submitted in Galgotias University, Greater Noida is an authentic record of my own work carried out during a period from 24/09/2018 to 16/6/2022 under the supervision of Dr. **Lokesh Varshney** (Supervisor).

The matter embodied in this thesis has not been submitted by me for the award of any other degree of this or any other University/Institute.

(Snigdha Sharma)

This is to certify that the above statement made by the candidate is correct to the best of our knowledge.

(**Dr. Lokesh Varshney)**
Supervisor
Deptt. of DEECE

The Ph.D. Viva-Voice examination of_____Research Scholar has been held on _____.

Sign. of Supervisor(s) Sign. of External Examiner

ABSTRACT

Nonrenewable sources of energy are inadequate to satisfy the electricity requirement with the rapid development of industries and other areas. Also, high consumption of these sources is inversely related to its life expectancy. Thus, non-conventional sources of energy play an essential part in generating electricity. Among all non-conventional resources, solar power is significant as it is clean energy source, easily and freely available, requires lesser maintenance, ecofriendly and economical. The Photovoltaic (PV) cells are widely used all over the world to convert energy of sun into electricity. The functioning of system is concerned by elements like irradiation, temperature rise, array topologies and shading effects on panels.

The intent of my work is inspecting and amplify yield of operating solar systems. Two of the major concerns in solar array due to partial shading are: Increase in Mismatch Losses (ML) and decrease in efficiency. The complete PV array system is concerned negatively with regard to efficiency by a little measure of shading on the PV module. The shading is the consequence of moving clouds, high rise buildings, long trees, shadow of one panel onto another etc. Due to this partial shading, many challenges occur in enhancing the performance of the PV solar array. The challenges include deviation of Maximum Power Point (MPP), power losses resulting in hot spot formation, degradation in power quality etc.

In this thesis, modeling of PV module is done using MATLAB/SIMULINK by combining subsystems of PV panel. The panels are then joined with each other in Series (S), Parallel (P) and Series Parallel (SP) connections to form an array. Different configurations have been implemented on PV solar array to observe their performance at different shading scenarios. The performance of these topologies has been highlighted with respect power obtained, losses because of shading, Fill Factor (FF) and overall efficiency of solar system. Simulated way is utilized to explain the functioning and estimation of all topologies. The electrical characteristics are also obtained by MATLAB. As per data achieved, Magic Square (MS) method have obtained highest power among all topologies.

ACKNOWLEDGEMENTS

Continuous efforts are one of the key parts while enduring the research work and this is impossible without the support and guidance which was obtained from many people and experts in research area.

Firstly, I would convey my gratitude to my supervisor, Dr. Lokesh Varshney for the helpful guidance and consistent support during my PhD study. His vast knowledge and extensive experience have motivated me every time of my scholarly work.

My appreciation also goes out to my Doctoral progress committee members for their valuable guidance and thoughts based on their area of expertise and experience all time my research period. I am also grateful to them for being collaborative in adjusting their suitable dates for progress review.

It was real pleasure for me to selected in PhD program from Galgotias University. I would like to thank Prof. (Dr.) Baibaswata Mahapatra, Dean, Department of Electrical, Electronics and Communication Engineering for help and support. I would also like to thank Dr. Preeti Bajaj, Vice-Chancellor, Dr. Naresh Kumar, Dean research, Head of Department, Ph.D Coordinator and all staff members for making me understand various guidelines of program and make me to achieve on time.

I want to thank Prof. (Dr.) R.K. Saket, Indian Institute of Technology for providing beneficial guidance for writing research paper and providing his vast knowledge and extensive experience in the research work field. His valuable advices proved to be very beneficial in clearing concepts, writing research papers and to follow the correct path.

The team of people with the greatest indirect contribution to this work is my mother, father and my mother-in-law, father-in law. They have really supported and barred me specially during last three years of research period. It would have been impossible to carry out this research work without them. They have made numerous sacrifices to make me achieve this.

In the last but most important person in my life my husband Roopendra Upadhyay who has given strength me during my research work. He has spent night on night in giving me guidance and helping me in guiding me his presentation techniques. It was a great work done by him.

Finally, I express my thanks to almighty GOD for driving me all the way and listening my prayers in difficult times to give strength to come out within situation.

Greater Noida 2022 **(Snigdha Sharma)**

TABLE OF CONTENTS

LIST OF FIGURES

LIST OF TABLES

LIST OF ABBREVIATIONS AND SYMBOLS

ABBREVIATIONS

PV	Photovoltaic
ML	Mismatch Losses
MPP	Maximum Power Point
S	Series
P	Parallel
SP	Series Parallel
FF	Fill Factor
MS	Magic Square
PSO	Particle Swarm Optimization
TCT	Total Cross Tied
BL	Bridge Link
HC	Honey Comb
NS	Non-Symmetrical
LS	Latin Square
PRM-FEC	Physical Relocation of Module with Fixed Electrical Connections
NREL	National Renewable Energy Laboratory
GMPP	Global Maximum Power Point
RM	Reconfigured Method
LD	Ladder
OE	Odd/Even
DS	Dominance Square
CS	Competence Square
SN	Short Narrow
SW	Short Wide
LN	Long Narrow

LW	Long Wide
GMPPSTC	Global Maximum Power Point at Standard Test Condition
GMPPPS	Global Maximum Power Point at Partial Shading
PS	Partial Shading

SYMBOLS

I	Current (A)
V	Voltage (V)
P	Power (P)
J	Net Current (A)
JL	Light Generated Current Density (A/m^2)
Ji	Normal Diode Current Density (A/m^2)
Jo	Output Current Density (A/m^2)
Voc	Open Circuit Votage (V)
Q	Electron Charge (C)
Is	Short Circuit Current (A)
Ks	Short Circuit Current of a Cell at Standard Test Condition (A)
D	Ideality Factor of Diode
Eg0	Band Gap Energy of Semiconductor (eV)
IRD	Solar Irradiation (W/m^2)
ISTC	Solar Irradiation at Standard Test Condition (W/m^2)
Kb	Boltzmann's Constant (J/K)
N	Number of Series Cells
Rse	Series Resistance (Ω)
Tn	Nominal Temperature (K)
To	Operating Temperature (K)
Rsh	Shunt Resistance (Ω)
Pmax	Maximum Power (W)
Vmp	Maximum Voltage (V)

Imp	Maximum Current (A)
Jmp	Maximum Current Density (A/m^2)
Psun	Total Power Density of Sunlight (W/m^2)
H	Efficiency
Ip	Photocurrent (A)
Io	Saturation Current (A)
Ir	Reverse Saturation Current (A)
Ish	Shunt Current (A)
I	Output Current (A)
R	Total Number of Rows
H	Total Number of Rows/2
I	Element of a Row
I_R	Row Current (A)
I_m	Module Current (A)

LIST OF PUBLICATIONS

During this Ph.D., I published and communicated six papers in different journals and conferences. This section presents the detail of research articles published during this Ph. D., which are listed below.

1) Comparative Evaluation of Novel Configurations Under Shading Conditions published in Journal of Electrical Systems (JES), Vol. 18, Issue 1, 2022, pp. 97-108, E-SCI Indexed Journal.

2) Performance Enhancement of PV System Configurations Under Partial Shading Conditions Using MS Method published in IEEE ACCESS, Vol. 9, 2021, pp. 56630-56644, SCI Indexed Journal.

3) Increasing the Efficiency of Solar PV Array Using Sudoku Configuration, International Conference on Advance Computing and Innovative Technologies in Engineering (ICACITE), 4-5 March 2021, SCOPUS Indexed Conference.

4) Analysis and Comparison of PV Array MPPT Techniques to Increase Output Power, International Conference on Advance Computing and Innovative Technologies in Engineering (ICACITE), 4-5 March 2021, SCOPUS Indexed Conference.

5) Comprehension of Different Techniques Used in Increasing Output of Photovoltaic System, International Conference on Electrical and Electronics Engineering (ICEEE), 21-22 Feburary 2020, published in Lecture Notes in Electrical Engineering book series (LNEE), Vol. 661, pp. 203-218, SCOPUS Indexed Conference.

6) Analysis of Equipment Sizing and Designing of 132/33/11KV Substation, IEEE International Students' Conference on Electrical, Electronics and Computer Science (SCEECS), 22-23 Feburary 2020, SCOPUS Indexed Conference.

CHAPTER 1

INTRODUCTION

1.1 Introduction

The non-renewable energy reserves in generating power causes greenhouse gas emission and environmental problems. This motivates the adoption of sustainable energy for bulk production of electricity. Among all renewable resources, solar energy is used due to its abundancy, clean production etc. Photovoltaic (PV) cells are major component for generation of power from solar energy which includes two steps: first one is absorption of beam as well as diffuse solar radiations and another step is to transform sun beams into electricity. The array supplies output power by solar power system which is presented by figure 1.1.

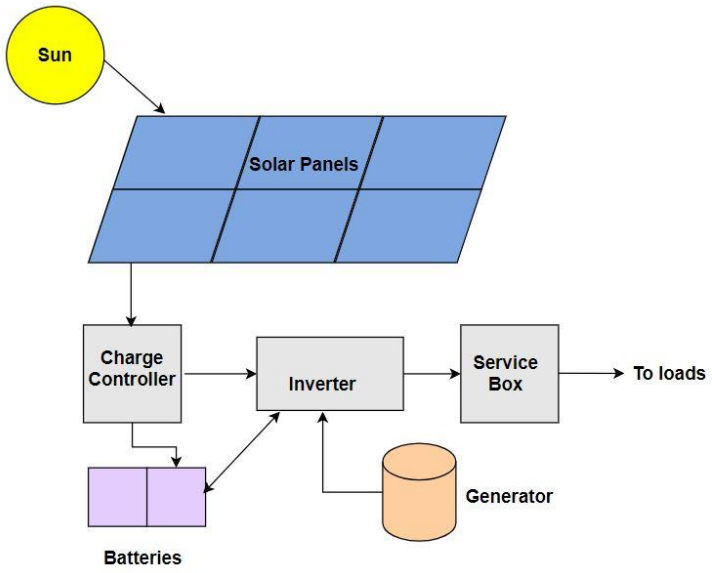

Figure 1.1 Solar Power System

The PV panels receive incident radiations from the sun and transform into electrical energy. The output of panels is taken by charge controller which controls battery charging. Batteries are used to store dc power from solar panels. Batteries provide dc power to inverter which transits dc to ac which is suitable for load. The service box contains circuit breakers used to protect the overall PV system. Generator is used as an alternative in case of cloudy or rainy atmosphere or when batteries are not charged.

Along with the alteration in sunbeams strength, load characteristic of solar PV network under concerned varies to keep yielded power maximum. These characteristics get complicated with the increase in shading scenarios. The I-V curve can be determined by final equivalent of PV cell as presented in figure 1.2.

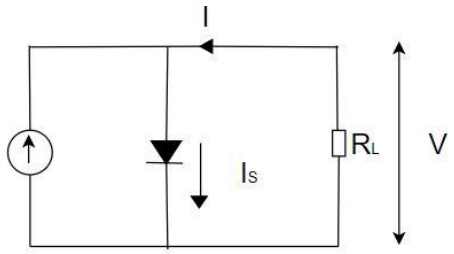

Figure 1.2 Final Equivalent Circuit

Let us consider an array of 1 Soltech 1STH-215-P which includes 10 series panels and 40 parallel cords. The electrical curves of the given model are shown by figure 1.3 at different temperatures.

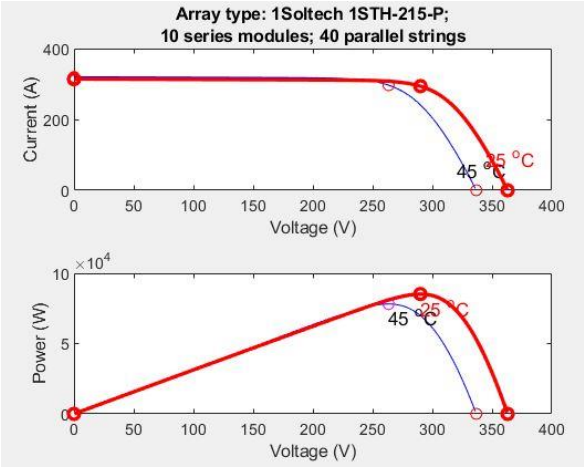

Figure 1.3 Electrical Characteristics of an Array

1.2 Overview of Thesis

Chapter 2 provides a literature survey on different aspects of solar array topologies. The thesis includes the study of aspects which affects the execution of solar PV system are shading effects, temperature, Mismatch Losses (ML), Fill Factor (FF)etc. The review is used to determine the objectives of thesis.

Chapter 3 represents the equivalent circuit and simulated model of PV module. It contains five different models of PV array subsystems - photocurrent, reverse saturation current, saturation current, shunt current and final output current. The chapter also includes electrical characteristics of PV array.

Chapter 4 represents detailed study different types of configurations which is mainly categorized into three classifications – Conventional, Hybrid and Puzzle based configurations. It is seen from study that puzzle based configurations are beneficial than remaining classifications. The chapter also contains pros and cons of all configurations.

Chapter 5 explain the significance of analysis of topologies at various shading scenarios. It consists of causes and effect of different shading conditions on various topologies. For verification of results, models of configurations are created and simulated under MATLAB/SIMULINK environment.

Chapter 6 introduces the conclusion and future scope of the thesis investigations.

1.3 Thesis Objective

The aim of my work is to inspect and increase the yield of already operating solar systems. In addition, different classifications of configurations and shading conditions have been studied to determine the most advantageous scenario. The analysis is done finally to obtain the results based on performance and validated using MATLAB/SIMULINK software. Four of the major concerns in solar array due to partial shading are:

- Mismatch losses
- Output power
- Fill Factor
- Efficiency

CHAPTER 2

LITERATURE REVIEW

The authors of paper [1] investigated an algorithm which is obtained by variant of Particle Swarm Optimization (PSO) for tracking Maximum Power Point (MPP) accurately. This adaptive perceptive PSO has been validated by hardware as well as software implementation on multiple solar PV arrays. The paper [2] provides a model which is used to determine the shading estimate of solar PV arrays. This mathematical model does not require complete current vs voltage characteristics but it requires power for estimation. Y. J. Wang et al. [3] proposed an analytical model which contains various orientation and shades of PV panels. The effects of these orientations and shades on electrical characteristics are studied in this paper. It also includes the study of effect of reverse voltage on solar PV panel. The authors of paper [4] analyzed different configurations used to carry out the analysis. It is validated that with overlapped diodes, losses in panels are one third of its maximum power while in case of without overlapped diodes, losses occur only due to diode power consumption. The paper [5] presents a model using PSCAD under unshaded panels as well as partially shaded panels. Experimental data is used for verifying the simulation results. The farms based on solar PV array [6] has certain requirements such as less amount of shading, reduced current and increased voltage. The novel farm configuration includes all these modified parameters to provide better results. Different configurations are compared and evaluated for calculating the performance of each topology. The results are validated by simulation. A new simulator model in [7] is proposed along with two diodes for determining solar PV cell. Four parameters are calculated to decrease computational time. Five different panels are used to validate the accuracy of simulator. This simulator easily supports MPP chasing algorithms in addition to converters. The authors of paper [8] considers series PV array which contains 18 panels joined in series. Electrical characteristics has been studied for the solar PV system at shading scenarios. Experimental values are taken into account for verifying simulated model. The paper [9] analyzes the behavior of series and parallel configurations using Brune's conditions. Lab view is used to verify the results. Also, a simulator is designed to estimate the parameters of PV network. An array in [10] is developed using MATLAB/SIMULINK to determine the behavior of

electrical characteristics. Also, another model is integrated with electronic circuit to determine the performance of circuit. The theoretical results are verified by experimental results.

Anssi Maki et al. [11] proposed a simulation model of series and parallel connections in order to calculate the mismatch losses. Under shading scenario, the individual short strings performs better than long series strings. Also, lesser mismatch losses occur in separate short strings. The authors of paper [12] presents distinct PV classifications under many shading conditions. A code of MATLAB is developed to determine measure of an array, classification of topology and total bypass diodes. The paper [13] gives an analytical comparison between SP and Total Cross Tied (TCT) topologies. The piecewise linear parallel branches method is also included for simulation purpose. The problem of shading produces very strong impact on solar PV panels. To minimize this problem, the authors of [14] study available configurations under shading conditions along with their effect on output power. The paper [15] investigated an easy PV model which can determine its parameters. The algorithm is observed by both experimental as well as by simulation to estimate the total power produced. Cell level analysis is done in [16] and it considers full as well as half size PV cells. SPICE software has been used for implementing an equivalent circuit of a cell. Three topologies have been considered for cell-based analysis in which SP connection proves that power produced is better under shading condition. The paper [17] proposed a multidimensional configuration that is very effective in cost of solar PV array. The control system used will be benefitted by lesser sensors as well as transducers by using aforementioned configuration. The current and power curves of solar PV systems are shown by final results. The authors of paper [18] considers four panels array which undergoes three different circumstances. The first condition which is applied on an array is same temperature and different solar irradiance. Second condition is at same solar irradiance and different temperature and last condition is at different solar irradiance as well as different temperature. Electrical characteristics are determined for each case and verified the theoretical values by using experimental analysis. The series mathematical model is presented in [19] to determine the output of solar PV system. Three factors have been applied to the model to extract accurate output. The first condition is to alter the avalanche effect for including a parameter which is a function of shaded and un shaded solar cells. The second condition is to insert a resistance to show the effect of variable current and the last condition is to add a voltage source to minimize the variation in current near open circuit voltage. The results are compared with observed data which verifies that root mean square error comes less

than 2.37%. The authors of [20] provides an elaborated analysis on TCT model of a solar PV array. Array voltages and electrical characteristics have been calculated using the aforementioned model. The verification of simulated results is done experimentally.

Bishop modelling based model is given by the authors of [21] to calculate the performance of electrical characteristics of a solar PV array. The SP connection is taken into consideration along with bypass diode. The model is used for total analysis of array voltage, array current and power under various shading scenarios. The paper [22] proposed a heuristic mode for calculating electrical characteristics of series PV system. The experimental values are in contrast with theoretical values to measure the difference and to validate the results. The paper [23] investigated a new model which is established in MATLAB to compute parameters of solar PV array. The simulated model is compared with DeSoto model, INSEL and PV syst at distinct irradiance and temperature. Also, some factors are included which have an impact on the functioning of a system such as aging, soiling as well as derating. These factors are included for obtaining more realistic results. Three PV panels of short strings are taken into consideration in [24] in which series and parallel connection are compared under various degree of shading. The fill factor and power losses are determined in the article for short series as well as parallel strings. It is proved that short parallel string is better than short series string in case of applications which require less power. The paper [25] analyzes power losses under different shade patterns. Also, power peaks are determined which comes within 5% of true values under every case. F. Belhachat et al. [26] examined the efficiency of an array configurations at different shading scenarios. The bishop model is used to describe the performance of negative voltage is taken and implemented using Simulink. According to the results obtained, TCT is superior in contrast to other configurations. The authors of [27] examined the effect of size of PV array, various topologies and shading pattern over total energy yield at shading conditions in detail. The paper [28] represents a method to extract electrical characteristics of PV system, either regular or irregular. The proposed method describes lesser number of equations used for drawing electrical curves. Bypass diode are taken in antiparallel with each panel and results are obtained using MATLAB/Simulink software. The multicrystalline PV panel is taken in [29] for describing the behavior of series, parallel and SP connections. Two conditions – homogeneous and heterogeneous are applied on PV panel to extract their electrical characteristics. The analysis has been done on array with different configurations along with bypass diodes. The results show that final power enhances in case of parallel connection under shading scenario.

Reconfiguration approach is taken in [30] for SP configuration under shading conditions. Further, rough sets theory-based algorithm is used for fast controlling purpose. The aforementioned theory defines the behavior of reconfiguration approach. Both simulated and experiment data are used to provide the effective results.

The paper [31] investigated an optimized algorithm for examining the best configuration. This procedure is valid for real time PV applications and requires easy mathematical steps for calculations. It is verified by the results that there is less computational burden while using the aforementioned algorithm. The authors of [32] devoted to the optimized method for better configuration of an array under different patterns. The simulated and real values are compared to determine the performance of PV array. SPICE software is used for simulation purpose. Results shows that there is 4-6% enhancement in output power. A novel pattern that is Futoshiki pattern is presented in [33] which is based on puzzle. This method enhances power and reduces power losses with respect to TCT under various operating conditions. The simulated as well as experimental data are compared for verifying the results. The paper [34] analyzed 2x2 TCT topology under different operating conditions. By simulations in MATLAB, TCT overcomes the performance of remaining configurations. The authors of paper [35] proposed a comprehensive study between conventional and puzzle-based configurations. In this paper, Non-Symmetrical (NS) configuration is described and analyzed under different operating conditions. Simulation results are carried out for analyzing the behavior of all configurations. The results reported that proposed topology is higher with respect to output power in some cases. The shading effect is studied in [36-37] in terms of electrical graphs. Results are obtained by simulation which proves that TCT along with incremental conductance method is superior to SP with incremental conductance. A. S. Yadav et al. [38] represents performance enhancement in reconfigurations with reference to existing topologies. The 4x4 matrix is taken for all configurations under various shading scenarios. The reconfigure topology is superior in some cases of shading than conventional configurations. The paper [39] presents electrical characteristics of series, parallel and SP configuration. The obtained results verifies that parallel connection performs well under uniform as well as non-uniform conditions. The submodule model is detected in [40] for extracting electrical curves of SP configuration. Bisection procedure is used for solving PV equations. The power losses are determined experimentally after many years of environmental exposure.

The authors of paper [41] determined uniform as well as non-uniform shading impact on solar PV array. Random shade is applied practically on an array to observe the enactment of PV array. The results are significant in achieving the design and working of an array at different shading scenarios. The paper [42] presents three novel configurations to minimize effect of shading. The aforementioned configurations are compared with conventional configurations. The final power of novel configurations enhances by 19%-40% of SP and 13%-68% of TCT. A cross diagonal view configuration is investigated in [43] to spread the shade over an entire array. The procedure is superior to other configurations and provides power enhancement of 23.9%. Smita Pareek et al. [44] presents the effect of conventional configurations on MPP under different shading situations. The proposed interconnection has benefits such as less mismatch losses, simple, cost of installation and wiring is minimized. The paper [45] examine sensitivity of solar PV array which includes an algorithm for obtaining highest power for all shading patterns. The optimized connection method is implemented on small and large PV array of 3x3 and 7x7 matrix respectively. The results highlight power generated in contrast to previous schemes. Sub-module integrated converter-based configuration is investigated in [46] for extracting solar energy. This procedure is beneficial in respect of cost, execution and productiveness. The results declare their merits as compared to other configurations. The authors of [47] proposed the module based on Fibonacci includes lot of factors like more stages, light reflection from one panel to other, less amount of shading and effect of cell shade on another cell. Authors acquaint the new arrangement of Fibonacci mode which depends upon HC design for attaining electrical characteristics. The paper [48] uses Fibonacci based panels via Simulink as well as experimental. The power generation increases by installing aforementioned modules. The work in [49] discusses the effect of short circuit on SP array. This paper focusses on current vs voltage characteristics and degree of homogeneity. This is beneficial in obtaining effect of modules failure without extracting information about system. The optimized configuration is detected in [50] via particle swarm optimization procedure. The switch set configuration is determined for reconfiguration purpose. The outcome of using aforementioned procedure results in better operation under abnormal operating conditions with lesser number of switches.

The authors of [51] analyzes all conventional topologies. By PSIM, TCT obtain greatest power among all scenarios. The paper [52] investigated an energy storage model topology to enable stability in power fluctuation in solar PV system. The simulated model is checked and

verified before and after installation of storing devices. The storage model is economic as well as requires less investment. The behavior of electrical curves is identified in [53] by a trust region dogleg procedure at abnormal conditions. This method doesn't require many models to examine various topologies. The paper [54] focusses on a novel Latin Square (LS) pattern for spreading the shading on an entire array so that power losses can be minimized, and output power can be enhanced. By this method, multiple peaks can be reduced and an algorithm is used for achieving maximum power point. The analytical procedure based on model is described in [55] for chasing MPP at shading scenarios. The experimental data is compared with theoretical values for verification of results. The estimation error is also determined and thus, array performance can be observed more accurately. A novel magic square topology is presented in [56] to obtain greater power as output in a solar PV array. The comparison is made among TCT, SuDoKu and MS at various shading patterns. As per proposed procedure, all the strings contribute in generating power and global peak is shifted towards the operating point. The overall performance enhances using MS method. The authors of paper [57] investigated competence square method which is a puzzle-based pattern for relocation of modules. Four shading scenarios are considered and implemented on configurations to obtain results. The proposed technique shows eminence in achieving good electrical characteristics, enhanced fill factor, enhanced power and high energy savings. The global maximum power point behavior has been studied and analyzed in [58]. The analyzation procedure is carried out under different transitions due to movement of clouds. C. W. Hansen et al. [59] investigated a method for calculating the value of series resistance along with other factors for a PV model. The error is also found in order to make results more reliable and accurate. The authors of [60] presents expansion of a mathematical block for showing PV generator in ATP Draw. The manufacturer's datasheet is used for obtaining data regarding PV panel. The PV generator results are achieved by varying temperature, irradiance, series resistance, parallel resistance and SP panels.

The paper [61] deeply analyze auto reconfiguration method on 3x3 solar PV array. It is considered that the shading is progressively enhancing, thus three increasing order shading patterns are taken. Further, simulation is done for comparing results with practical data and making output more accurate. The authors of [62] presents advanced SuDoKu pattern to increase an array performance at various shading scenarios. The global MPP, FF, power losses and efficiency are calculated theoretically and results obtained shows improvement in performance. The panels are

reconfigured in [63] by using a structuring method at shading conditions. The array is structured using Odd/Even pattern in this paper. This method minimized the repeated local peaks so does not require an additional algorithm for tracking MPP. The authors of paper [64] gives extensive comparison among conventional topologies at artificial as well as real shading condition. Thermal voltage, FF, power losses and output power are the factors taken for analysis. The paper considers single diode PV panel for analyzation. Results provides better topology for a particular shade scenario. A novel skyscraper pattern was developed in [65] for dispersing shade on overall solar PV array. Both experimental as well as simulated values are observed and compared for calculating accuracy of results. According to results obtained, skyscraper method gives less mismatch losses and enhanced power output. The authors of [66] used conventional configurations at ideal switch case and non-ideal switch case. The total switch gets minimized for enhancing output power and reducing power losses. Manjunath et al. [67] presents increase in solar PV array performance at shading conditions. Odd/Even and SuDoKu methods are taken for comparative analysis with proposed technique. The reconfiguration techniques are investigated in [68] under different shading scenarios. These techniques are discussed under both static and dynamic cases on hardware. The observed data shows that costly dynamic mode overcomes static mode with respect to performance. The author of [69-70] focused on optimal SuDoKu method based on reconfiguration for 9x9 solar PV array. The aforementioned pattern is compared with SuDoKu pattern and the outcome is that proposed method is superior to SuDoKu pattern.

The work in [71] presents topologies with different categories of bypass diodes. Six categories are discussed and evaluated in order to obtain electrical curves for describing the detail behavior of an array. The SP connection is taken and all categories of bypass diode are implemented on it. According to the observed results multi-level octal bypass diode on SP configuration gives better performance among all topologies. The paper [72] focused on conventional topologies. This paper also describes hybrid configurations. The power gain is maximum in TCT topology as compared to rest of the topologies. The fault analysis is carried out in [73] via reconfiguration technique along with three conventional configurations. The comparison is made between polycrystalline technique and copper indium gallium selenide technique under different fault scenarios. The optimal method along with copper indium gallium selenide gives output with more power and a smaller number of peaks. The authors of [74] implemented reconfiguration technique on larger array of 9x9, 6x20, 16x16 and 25x25 at various

shading patterns. The proposed method boosts up the performance of all arrays. The hybrid SuDoKu configuration is investigated in [75] and comparative analysis is made with conventional topologies. The shading is considered due to moving clouds and their direction as well as speed is also taken into account for obtaining more practical output. The distributed maximum power point tracking is described in [76] for obtaining more power. The module integrated converter is applied on TCT topology. Also, cross coupling effect is reduced using aforementioned technique. The paper [77] gives review comprehensively of all topologies for solar PV array. This paper also includes merits and demerits of each technique described in the paper. The authors of [78] provides reconfiguration method in which power is directly evaluated for increasing power output. Theoretical as well as software values are observed, matched and validated for extracting the result of reconfiguration scheme. The paper [79] focusses on physical relocation and fixed column position of module with fixed electrical connections to minimize power losses under different shading conditions. The work in [80] discussed an algorithm to obtain only one peak by dispersing equal shaded panels in every row. Simulation has been carried out to prove the performance after algorithm is applied.

To minimize the impact of partial shading, comprehensive review is done in [81-82] which includes conventional, hybrid, puzzle based and metaheuristic approaches. The existing topologies merits and challenges are also emphasized and discussed in this paper. Rupendra Kumar Pachauri et al [83] presents Latin square reconfiguration method against conventional configurations using MATLAB/SIMULINK software under shadows. Also, the presented technique is compared experimentally with TCT and SuDoKu topologies. The authors of [84] investigated a technique for reducing impact of shadow on an array. It has been proved that presented mode gives 14% increase in power as compared to existing techniques. The paper [85] uses 5x5 array at various shadows and studied impact of shading on conventional topologies in MATLAB/SIMULINK. Mohammed Alkahtani et al [86] focusses on gene evolution algorithm on reconfiguring 2x4 array to build up the overall power of PV system. As per authors, power enhances by 11.42% in comparison to non-uniformly aged PV array. Hegazy Rezk et al [87] presents an algorithm to provide solution of reconfiguration technique at four shading conditions. The paper [88] investigates five configurations- TCT, SuDoKu, Futoshiki, L shape and After Reconfiguration under eight shading patterns on 4x4 PV array. The L shape topology provides better results when combined with after reconfiguration in MATLAB/SIMULINK and all configurations are

experimentally validated. The authors of [89] presents ken-ken puzzle arrangement which can track MPP easily and improves the output power by 10.85%. The authors consider five different configurations under four shading patterns on 4x4 PV array. The performance is observed by parameters FF, ML and power loss. The paper [90] present an electronic circuit for reconfiguring bypass PV panels. The modules are firstly joined in SP connection and then reconfigured using electronic devices. The authors of [91] considers three patterns of shading on four different configurations. The topologies used in this paper are – TCT, novel TCT, Shape Do Ku and symmetric matrix TCT. Using software results, it is proved that symmetric matrix puzzle is more effective than rest of the configurations. The alternative tri tie method is investigated in [92] which is matched with conventional configurations in regard with MPP and FF. It is observed that new method outperforms than other topologies. The exploration of [93-95] is to illuminate the features of various PV classifications with respect to output power, FF, ML and efficiency. The aim is to examine and extract the functioning of various configurations at different shading scenarios. The main issue that occurs in the way of PV network working is shadowing. The key to this difficulty is to reconfigure the modules for obtaining good results at shading scenarios. To make this succeed different configurations has been reviewed, evaluated and matched via MATLAB/SIMULINK. Software based path is taken to explain the functioning and examination of all topologies. As per data obtained, MS technique is highly efficient.

CHAPTER 3

PV MODULE MODELING

3.1 PV Cell

This chapter provides the outline of PV module modeling. Different factors which are having impact on PV module have been postulated in the thesis. The variation of electrical characteristics with respect to different operating scenarios are simulated and analyzed. The design of solar PV system can be done using modeling and simulation. However, its design has certain limitations and challenges such as area required for installation, variation in solar irradiance, rise in temperature and PV products availability.

Basically, a PV cell is used for converting solar radiations directly into electrical energy. The PV cells has inherent property of photovoltaic effect which is responsible for absorbing photons and releasing electrons. These free electrons result in the flow of electric current. As PV cells are not heat engines so does not require high temperature rather room temperature is sufficient for their operation. The real efficiency of solar cell falls rapidly with the rise in temperature. Many cells are concatenated in series and are frame mounted to make a PV panel which was first created by Bell Laboratories in 1954. Large number of panels are stringed in S, P or SP combinations to make an array. The connection of array depends on the requirement of current and voltage. The figure 3.1 shows solar cell, module, and array.

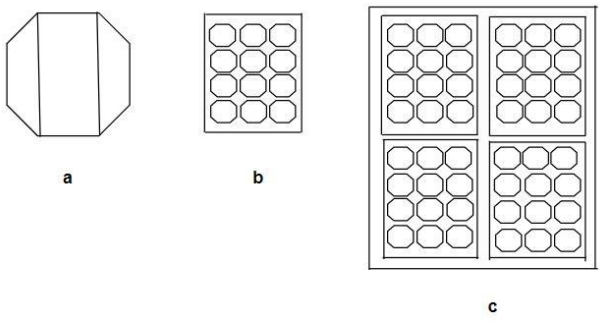

Figure 3.1 (a) Solar Cell (b) PV Module (c) PV Array

The solar cells are consisted of different materials in a distinct way. The most widely used material is silicon which is a semiconductor material. Mainly there are three types of technologies responsible for the formation of PV cell. The technologies classifications are shown in figure 3.2.

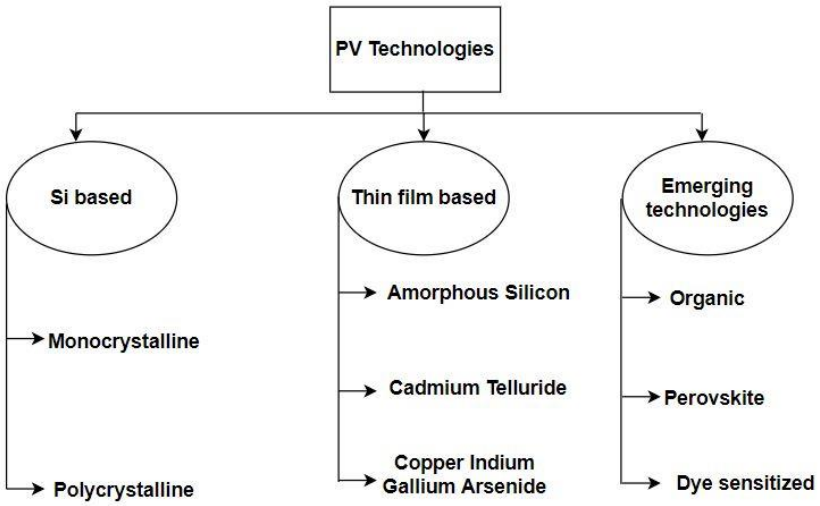

Figure 3.2. PV Technologies Classifications

3.1.1 Silicon based Technologies

3.1.1.1 Monocrystalline PV cells: The monocrystalline cells are manufactured from single crystal pure silicon. They have clipped corners, greater thickness, rigid, fragile and of black color. A single crystal is dipped into liquid silicon forming a cylindrical shape and pulled out. This crystal is then cut into thin wafers of silicon and an anti-reflecting coating is applied on the silicon wafer to form a monocrystalline cell. These cells have greater efficiency, long life, works at high temperature but it is costly and has slow process.

3.1.1.2 Polycrystalline PV cells: These cells do not require single crystal rather it requires many crystal grains of silicon in one solar PV cell. The number of silicon crystal fragments are melted and cut to form wafers. Their shining blue color makes them attractive. This technology makes PV cell more environment friendly than monocrystalline. They operate within temperature range of -40 ^{o}C to 85 ^{o}C and are simple and cheap. They have certain demerits such as their efficiency is low, and they are not long lasting as compared to monocrystalline cells.

3.1.2 Thin Film based Technologies

This technique contains many thin films of PV material on substrate. Different materials are used in this for absorbing maximum amount of light. Most widely used materials are as follows:

3.1.2.1 Amorphous silicon: It has p-i-n structure in which i indicates intrinsic layer of amorphous silicon. This is silicon allotropic form in which less amount of silicon is required in comparison to silicon-based technologies which leads to low cost. This material is nontoxic, abundantly available, and good in absorbing a wide range of light including even weak light spectrum. Due to lower fraction of silicon in this technology, its efficiency decreases.

3.1.2.2 Cadmium telluride: This contains p doped cadmium telluride along with n type cadmium sulphide heterojunction form. This material is toxic so needs prevention methods while manufacturing. It is beneficial in terms of less price for manufacturing.

3.1.2.3 Copper Indium Gallium Arsenide: This contains layers of copper, indium, gallium and selenide fabricated on substrate. In this, very thin layer is needed due to higher absorption capacity with respect to other materials.

3.1.3 Emerging Technologies

Some thin film technologies are considered as emerging technologies by National Renewable Energy Laboratory (NREL) due to non-implementation in practical applications and ongoing research in this field.

3.1.3.1 Organic: This technique is subjected to organic electronics which consists of organic polymers. These types of PV cells are light in weigh, enhancing efficiency, lifelong performance and flexible. They confront problems regarding stability and degradation.

3.1.3.2 Perovskite: This technique deals with perovskite compound based on halide elements. They require lead which is cheaper and easily available as well as ultra-thin layers for absorbing solar radiations. The only problems in this are lack of stability and fast degradation of material.

3.1.3.3 Dye sensitized: This technique uses photoelectrochemical system which includes an anode and an electrolyte. This material is semi flexible, less costly, and easy formation. They are having drawbacks such as lack of chemical stability and not easily available.

3.2 Equivalent Circuit of Solar Cell

A PV cell is generally using a p and n type semiconductors for making its physical configuration. Current and voltage relationship is given by

$$Ji = Jo[\exp\left(\frac{Ve}{KbTo}\right) - 1] \quad (1)$$

When junction receives sunbeams, electron hole pairs are formed leading to flow of current. The final current is obtained by subtracting light generated current from normal diode current. Figure 3.3 shows solar cell equivalent circuit. JL acts as a current source and net current J is given by

$$J = JL - Ji = JL - Jo[\exp\left(\frac{VQ}{KbTo}\right) - 1] \quad (2)$$

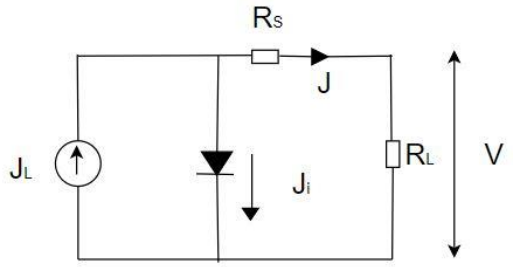

Figure 3.3 Equivalent Circuit of a Solar Cell

Reduction can be done in the cell voltage drop and internal resistance for an ideal cell is assumed to be zero i.e., Rs = 0. Figure 3.4 provides current density vs voltage plot. The open circuit voltage Voc for the ideal cell is then given by

$$Voc = \left(\frac{KbTo}{Q}\right) \ln\left[\frac{JL}{Jo} + 1\right] \quad (3)$$

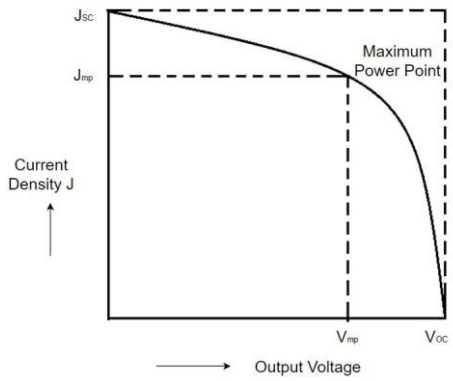

Figure 3.4. A Typical J-V Plot of Ideal Solar Cell

As JL>>Jo, Voc will be

$$Voc = \frac{KbTo}{Q} ln \frac{JL}{Jo} \quad (4)$$

The maximum power is given by

$$Pmax = Vmp.Jmp \quad (5)$$

The maximum efficiency is given by

$$\eta = \frac{VmpJmp}{Psun} \quad (6)$$

3.3 Simulated Model of PV Module

The PV network contains five panels concatenated in series which leads to the formation of a cord and five of these strings makes a parallel connection. Thus, 5x5 PV system includes 25 panels and 4.5 kW power capacity. Table 3.1 gives description of PV panel. To the explain the properties and control of electrical curves, equation 7 to 11 are used here. These equations have an important part in the formation of a panel and giving electrical curves.

Table 3.1 PV Module Specifications

PV Model	TP 180
Module Dimension	1587mmx790mmx50mm
Module Weight	16kg
Pmax	180W
VMPP	35.8V
IMPP	5.03A
Voc	43.6V
Is	5.48A
Number of Cells	72

$$Ip = \frac{[Is+Ks(To-298)]IRD}{1000} \quad (7)$$

$$Io = Ir(To/Tn)^3 \exp\left(\frac{\left[Q.Eg0.\left(\frac{1}{Tn}-\frac{1}{T}\right)\right]}{D.Kb}\right) \quad (8)$$

$$Ir = \frac{Is}{\exp[(Q.Voc)/(D.N.Kb.To)]} - 1 \quad (9)$$

$$Ish = \frac{V+I.Rse}{Rsh} \quad (10)$$

$$I = Ip - Io\left[\frac{[Q.V+Q.I.Rse]}{D.Kb.N.To}\right] - Ish \quad (11)$$

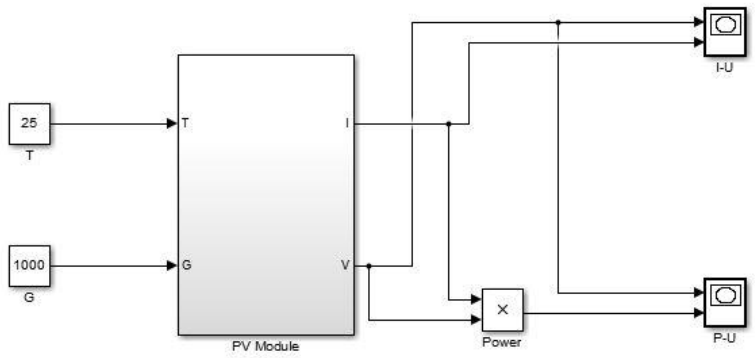

Figure 3.5 Simulated Circuit of PV Module

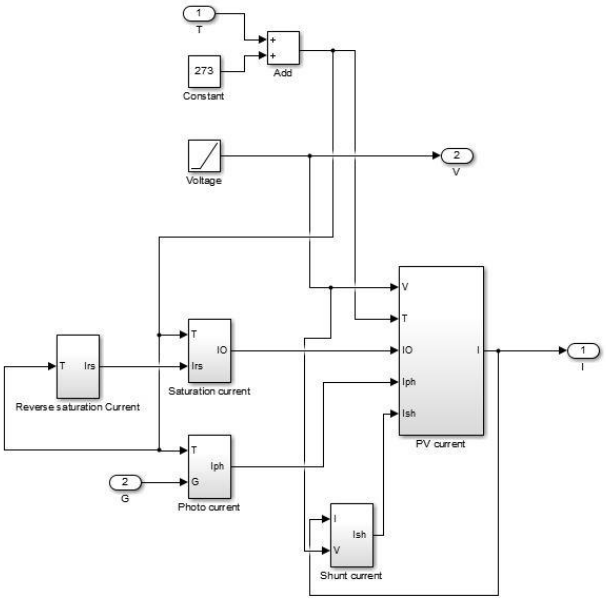

Figure 3.6 Subsystem of PV Module

The panel is illustrated and processed as indicated in figure 3.5. The subsystem is represented in figure 3.6. The electrical curves are presented by figure 3.7 and 3.8.

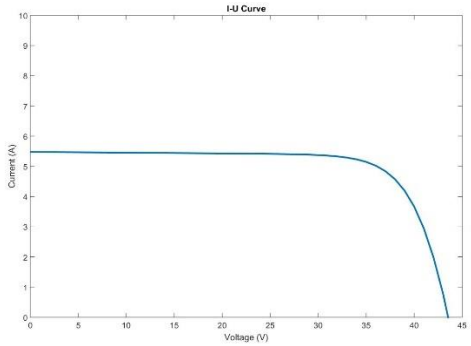

Figure 3.7 Simulated I-V Graph

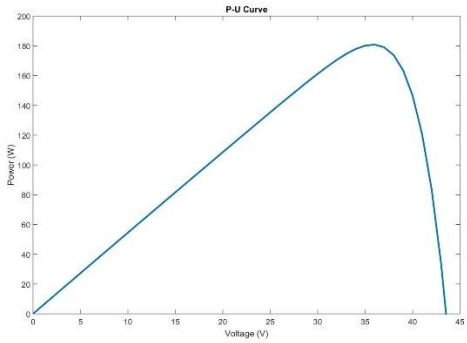

Figure 3.8 Simulated P-V Graph

CHAPTER 4

TYPES OF PV CONFIGURATIONS

Various types of PV topologies have been studied and examined under different shading scenarios. Figure 4.1 gives the brief introduction about various configurations based on different parameters – conventional configurations, hybrid configurations and puzzle-based configurations.

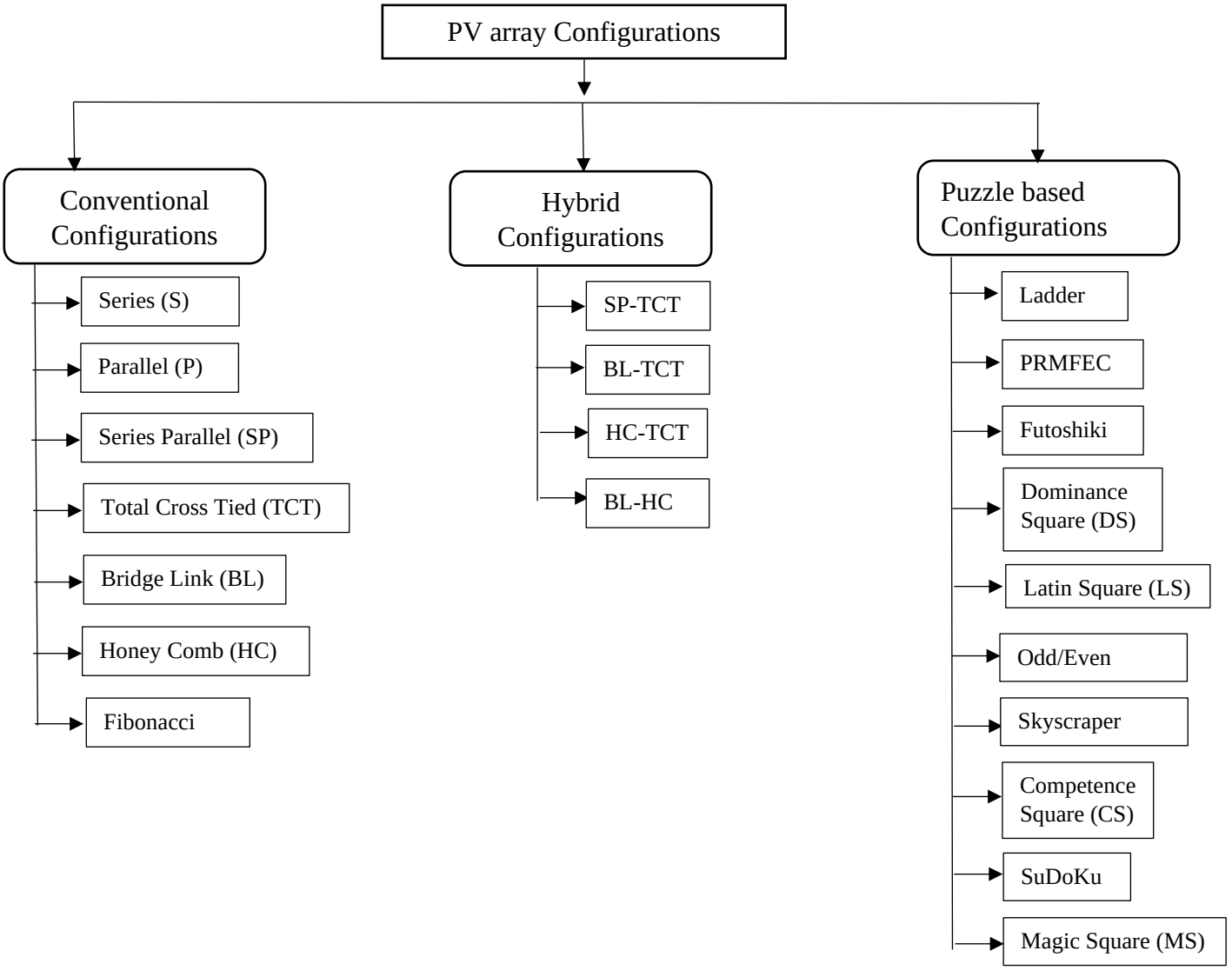

Figure 4.1 Categories of PV Array Topologies

4.1 Conventional Configurations

4.1.1 Series (S): The authors focused on the shadowing effect on electrical curves of a panel in series connection. It is noticed that shaded area of a module makes strong impact on behavior of electrical curves. Real time work is done in the paper [1] for series panels at different irradiation levels and temperature levels. The loss in power accounts for 22% for varying irradiance. The authors of [2] applied a model for showing the wellness of adopted model. In paper [4], 30 panels are taken into account which are in series connection at various shading conditions. The real time results depicts that the losses due to shading are dependent upon connection of bypass diode. Also, Global Maximum Power Point (GMPP) obtained highest peak at 70mW. The authors of [5] have taken 8 shading cases at irradiance from 130 to 992 W/m^2.

The performance analysis under distinct shadowing conditions is discussed in [8] which contains eighteen panels in series. The paper [9] provides a practical study based on 3 panels at distinct irradiance. By following this, the maximum value of GMPP is 180W. Both hardware and software-based study is performed in [10] by considering 3 panels in series connection at irradiation 220-890 W/m^2. Moreover, boost configuration is implemented for reducing error upto 0.56% in GMPP. The authors of [16] uses SP topology including 72 solar cells at non-uniform irradiation level. The simulated results depict that SP topology develops maximum power of 300W and minimum losses. 25 panels are considered in [17] for practical analysis under different shading cases. The authors of [23] proposed a practical set up under which 4 panels in series connection are compared with software results. Only 0.8 % error occurs between the two results. Similarly, in paper [28], 60 cells are considered under 25%, 50%, and 75% shading and their results are compared with experimental values for all shading scenarios. The series connection is presented in figure 4.2.

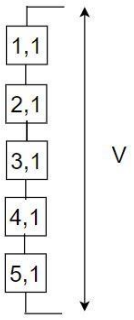

Figure 4.2 Series Configuration

4.1.2 Parallel (P): MATLAB/Simulink model has been applied in [1] for studying and analyzing the functioning of parallel connection. The authors of paper [9] uses a model containing 3, 4 and 8 panels for forming a configuration – SP, P and multi-string for evaluating the impact of shades on working of an array. The GMPP is maximum in SP topology. The simulated model is studied in [10-11] for examining 3x2 array which is connected in S and P topologies under all shading cases. The P configuration achieve GMPP of 2350 W at irradiance 132-729 W/m^2. A practical set up is implemented in [18] on 4 panels in three different configurations: S, P, SP. This is done to determine the functioning of PV system at various shading cases. The maximum GMPP is 954.88 W for P topology at irradiance 750 W/m^2-1160 W/m^2. The authors of [21] implemented 6x9 array for estimating impact of shading on S and P configuration at irradiance 100 W/m^2 to 1000 W/m^2. It is visible by results that P connection has highest GMPP. The parallel connection is presented in figure 4.3.

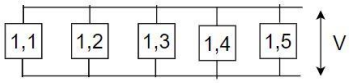

Figure 4.3 Parallel Configuration

4.1.3 Series Parallel (SP): By considering only S or P topology, it is almost impossible to enhance voltage and current range simultaneously. Thus, S and P together form SP which contains advantages of low price and losses. Five panels are joined in series creating cord and five of these cords are joined in parallel to extract SP topology as shown in figure 4.4. Many peaks occurred in case of series connection while single peak occurs in parallel

connection at shading conditions. SP is widely used topology as it is simple to implement. The whole power is improved but its performance is lacking under shadowing conditions.

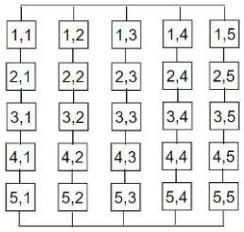

Figure 4.4 Series Parallel Configuration

The authors of [2] provides current experimental data based on hardware and software model. It contains a 3x3 and 4x4 array for analysis and the highest GMPP is 125W. The PV panel undergoes mathematical modeling in [19], which consider 4×3, 6×5, 6×6 PV array connected in SP configuration. The MPP is tracked at uniform irradiation for all the arrays. In addition to it, hardware-based calculation is also done to verify the software results. In paper [30], 2×2 and 2×3 arrays are taken in SP configuration via hardware. According to obtained results, the highest value of GMPP is 40W at insolation 100-1000 W/m^2.

4.1.4 Total Cross Tied (TCT): TCT connections are difficult to apply with respect to SP. It includes rows and columns which are crossly connected as depicted in figure 4.5. Various insolation's are also shown in the figure. TCT technique overcomes problems of SP configuration under shading scenarios but it goes through a disadvantage in case of total ties leading greater cable losses. TCT is divided into two categories: Bridge Link and Honey Comb.

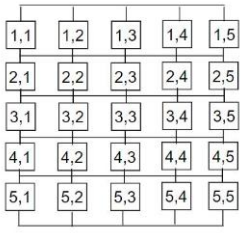

Figure 4.5 TCT Configuration

4.1.4.1. Bridge Linked (BL): BL is named so as it is based on bridge rectifier structure. It is one of the classifications of TCT which has overcome the drawback of a greater number of ties. It also has a merit of reduction in time of wire furnishing. Its drawback is that it severely affects total power at shade cases. The following connection is shown in figure 4.6.

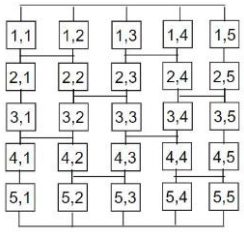

Figure 4.6 Bridge Link Connection

4.1.4.2. Honey Comb (HC): The HC is based on honeycomb structure. It is similar to BL except the connection of ties as shown in figure 4.7. It has a merit of lower output power losses and a disadvantage of unable to reduce power losses under all shading conditions.

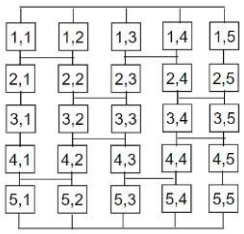

Figure 4.7 Honey Comb Configuration

The authors of [6] considered TCT which achieves highest GMPP of 1528W at solar irradiance 250- 1000 W/m^2. The array of 20x3 is taken in [7] for SP and TCT connections using MATLAB/Simulink and their performance are evaluated under varying irradiations. The 3x3 array is used for 4 conventional topologies in paper [14]. The authors of [20] uses simulated model of SP and TCT to check their performance under various shadows. The obtained results provide the GMPP data as 140W at at irradiation level as 332.63-560.60 W/m^2. The practical set up of BL and TCT is applied in [25] under 10 different shadowing effects. The hardware result clearly indicates that TCT has maximum GMPP of 678.40W at insolation of 289-992 W/m^2. The authors of [26] make a comprehensive study on various conventional configurations with respect to different

shading. The 6x4 array is considered for performance evaluation by taking into account the following features: output power, FF and voltage. The GMPP is 1446W for TCT at irradiation 300-1000 W/m^2. The reconfiguration-based configuration is considered along with conventional topologies to determine the GMPP. Five shading cases are taken to be implemented on all topologies and the highest GMPP of 180W is obtained for TCT connection. In [34], a 4x4 simulated model are considered under 2 different shades including five and four cases respectively. At 200-1000 W/m^2 irradiance, TCT is superior with respect to remaining configurations.

The authors of paper [53] uses experimental and simulated data for evaluating conventional configurations. The GMPP of 400W is verified for TCT configuration under all shading cases. The 3x3 array is taken in [61] for obtaining output power at irradiance of 380-710 W/m^2. The use of electromechanical relay and embedded system deals with the switching of SP to TCT. In [73], comprehensive study is done due to deficiency of non-uniform solar insolation of 400-1000 W/m^2. The multiple peak array case is evaluated based on different configurations.

4.1.5 Fibonacci: The panels based on Fibonacci number are plotted by the arrangement of leaves on plant. They have been presented as a way of fast collecting sun's energy all over the day. In a Fibonacci number of modules, it is necessary to connect the solar cells of each PV panel in series in order to obtain high output voltage. However, series connection of this type can also decrease the measure of electric power yielded by the Fibonacci number modules if the shadows produced by panels fall on those receiving sunlight. Basically, Fibonacci number PV modules is a structure in which PV panels are arranged like leaves of plants based on Fibonacci sequence. The angle between successive leaves is determined by phyllotaxis, which is expressed by the Fn term of Fibonacci sequence and term Fn+2 thereafter. The phyllotaxis of a Fibonacci number of PV modules is 1/3, 2/5, 3/8 and so on. The numerator of phyllotaxis represents number of leafs turns, and the denominator represents the number of leaves. The degree of opening in 1/3 leaf order is 1/3 * 360^o = 120^o. Figure 4.8 shows a schematic diagram of a Fibonacci number of PV modules in which six solar panels are attached to the center pole following the above mentioned phyllotaxis. Each solar cell panel has a sector shape with a center angle of 120^o. Previous reports have

shown that the amount of power generation of a Fibonacci number of PV modules per unit of installation area increases when compared to a conventional planar installation. More specifically, the quantity of power yielded for two exactly same levels with 1/3 phyllotaxis is 1.5 times that obtainable with a PV panel installation on a flat surface. A Fibonacci number of PV modules that mimics this leaf arrangement has the following features:

- The number of stages in the Fibonacci number PV modules system can be enhanced.
- Light reflected by the PV cell surface can also use via other PV cells.
- It is necessary to take into consideration the influence of the shadows the PV cells cast on each other.
- A Fibonacci number of PV modules is vegetation friendly because its reduced area means that it will cast less shadow on the area around it over course of the day and is thus suitable for solar sharing.

The biggest challenge facing Fibonacci number PV modules use is the reduction in power generation that occurs when the shadows of the upper-level solar panels fall on the lower panels.

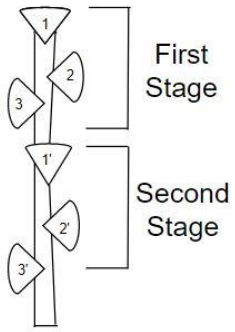

Figure 4.8 Fibonacci Number PV Modules

4.2 Hybrid Configurations

4.2.1 SP-TCT: In paper [35], software model is created and investigated for conventional and novel configurations. The 5×4 and 9×4 arrays are considered and as per results GMPP

is 2733W at 350-1000 W/m^2 irradiation for non-symmetric 1 (NS1) topology. Figure 4.9 shows the connection pattern of SP-TCT.

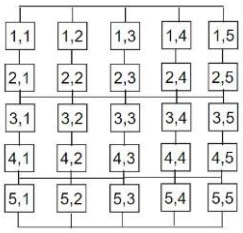

Figure 4.9 SP TCT Connection Pattern

4.2.2 BL-TCT: This configuration is novel in its kind and is formed by alternately connecting two columns of array in TCT configuration and next two columns in BL configuration. This is shown in figure 4.10. In 5x5 TCT PV configuration, the total number of cross ties are 16 which are more and hence requires more wires for connection. In this PV configuration an attempt is made to reduce the requirement of wires thereby reducing its complexity but still maintaining its performance better than BL and HC PV Configuration with respect to extracting largest power under shading cases and at par with TCT PV configuration.

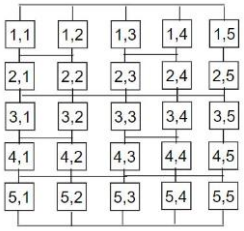

Figure 4.10 BL TCT Connection Pattern

4.2.3 HC-TCT: The modification of BL topology leads to HC topology HC-TCT which contains merits of TCT and HC. The TCT contains double number of ties as compared to HC. However, all modules in an array occupies same behavior and each topology provides same power in case of absence of mismatching. When mismatch occurs, one topology can perform well with respect to remaining topologies. The functioning of the HC method is matchable to TCT and hybrid configurations. HC sometimes act better than the other conventional configurations. For obtaining the wider view of HC array under shading cases, the mathematical evaluation is necessary at general operating conditions. Thus, the

focused 4 × 5 HC pattern is taken as shown in figure 4.11 for analysis. This concept can be widespread among all shading scenarios.

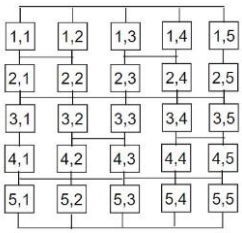

Figure 4.11 HC TCT Connection Pattern

4.2.4 BL-HC: The BLHC topology can minimize the demerits of other conventional configuration like lesser number of series panels. In this configuration, the panels are joined in a similar way as TCT except first-row panels. The panels are connected together for obtaining the required output voltage. The number of series panels got reduced than other conventional configurations. Thus, the mismatch losses are lower than others and somewhat greater than TCT connection. The simulated results provide electrical characteristics at different shadowing cases. Figure 4.12 shows the connection of BL-HC.

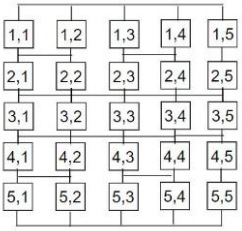

Figure 4.12 BL HC Connection Pattern

4.3 Puzzle based Configurations

4.3.1 Ladder (LD): In [72, 73, 75], in addition with conventional topologies, the paper has included ladder method as in figure 4.13 for functioning evaluation for irradiance from 300W/m^2 -1000W/m^2. The adequate performance index is noticed and seemed that hybrid and ladder topologies perform better at all environmental cases.

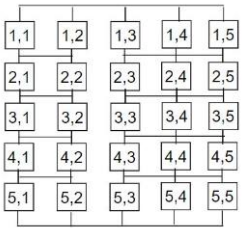

Figure 4.13 Ladder Configuration

The ladder pattern can defeat the demerits of bridge link and series parallel connections. The final structure seems as a ladder, thus named ladder configuration. The total current of PV system is addition of all module currents. This arrangement does not have any modules joined in series while rows are concatenated in series. Thus, the mismatch loss is lower than the bridge link, and series parallel and greater than TCT, honey comb and other hybrid topologies.

4.3.2 Physical Relocation of Module with Fixed Electrical Connections (PRM-FEC) Shade Dispersion Method: An advantage of shade spreading is taken care in this method. The spreading restricts large amount of shade in a single row or column. As far as connections are concerned, they are matched with the connections of TCT but panels are relocated to a new position. The shading panels along with shading scenarios that are different from TCT and SP are shown in figure 4.14. A problem that occurs in this method is complexity in implementation because of panels relocation which finally enhances the price of wires. This method uses algorithm based on odd row. To obtain the desired results, repetition of row elements or column elements are not considered in this method. The following steps are taken for creating PRM-FEC configuration which includes equations (1)-(25).

1,1	4,2	2,3	5,4	1,5
2,1	5,2	3,3	1,4	2,5
3,1	1,2	4,3	2,4	3,5
4,1	2,2	5,3	3,4	4,5
5,1	3,2	1,3	4,4	5,5

Figure 4.14 PRM-FEC Pattern

1. The data of 1st column is determined by equations (12)-(16).

$$Row1 = 1,1 \quad (12)$$

$$Row2 = 2,1 \quad (13)$$

$$Row3 = 3,1 \quad (14)$$

$$Row4 = 4,1 \quad (15)$$

$$Row5 = 5,1 \quad (16)$$

2. The data of 2nd column is determined by equations (17)-(21). Here h = r/2, r represents total rows and, i = 1, 2, 3, 4, 5.

$$Row1 = h+i,\ 2 = 4,2 \quad (17)$$

$$Row2 = h+i,\ 2 = 5,2 \quad (18)$$

$$Row3 = h+i-r,\ 2 = 1,2 \quad (19)$$

$$Row4 = h+i-r,\ 2 = 2,2 \quad (20)$$

$$Row5 = h+i-r,\ 2 = 3,2 \quad (21)$$

3. The data of 3rd column is determined by equations (22)-(26).

$$Row1 = 2,3 \quad (22)$$

$$Row2 = 3,3 \quad (23)$$

$$Row3 = 4,3 \quad (24)$$

$$Row4 = 5,3 \quad (25)$$

$$Row5 = 1,3 \quad (26)$$

4. The data of 4th column is determined by equations (27)-(31).

$$Row1 = 5,4 \quad (27)$$

$$Row2 = 1,4 \quad (28)$$

$$Row3 = 2,4 \quad (29)$$

$$Row4 = 3,4 \quad (30)$$

$$Row5 = 4,4 \quad (31)$$

5. The data of 5th column is determined by equations (32)-(36).

$$Row1 = 1,5 \quad (32)$$

$$Row2 = 2,5 \quad (33)$$

$$Row3 = 3,5 \quad (34)$$

$$Row4 = 4,5 \quad (35)$$

$$Row5 = 5,5 \quad (36)$$

4.3.3 Futoshiki: This is a logical puzzle which can be solved till 9x9 matrix. The comparing signs are used to calculate the elements of futoshiki. For obtaining the elements at primary stage, extract the digits using symbols in futoshiki puzzle. A 5x5 matrix is taken so a single sign of greater following next cell, then the highest cell should be 2,3,4,5 and lowest cell should be 1,2,3,4. The condition a>b>c is essential for obtaining the elements of puzzle. For example, if a is at 3 then c must not be > 3. The general rules of SuDoKu are also helpful in futoshiki pattern.

The evaluation of 5×5 and 4×4 arrays is done for TCT and futoshiki pattern at distinct shading transitions [33]. The results of configurations are calculated, compared and verified practically. The following method is described by figure 4.15.

1,1	4,2	3,3	5,4	2,5
2,1	5,2	4,3	3,4	1,5
3,1	2,2	5,3	1,4	4,5
5,1	1,2	2,3	4,4	3,5
4,1	3,2	1,3	2,4	5,5

Figure 4.15 Futoshiki Pattern

4.3.4 Dominance Square (DS): This method goes through dominant square pattern for placing the digits in the matrix. Dominance square is a logical puzzle that arranges letters and digits in sequence. In a 5x5 matrix, the sequence is given in figure 4.16. The placement of digits/alphabet in this method shown in figure 4.17. Four rules are necessary for determining the elements of DS. They are:

1: As per this step, the alphabets are placed in diagonal position with respect to its previous place. The starting place a11 can be randomly selected in any row in third column. In this thesis, the starting position is implemented at fourth row for all shading scenarios.

2: Now after applying first step if there is a limit extension of column then the locations sequence will get resume from the consecutive column. The sequence of row during this procedure remains same.

3: In case there is a limit extension of row, then location sequence starts from successive row. The sequence of column during this procedure remains same.

4: Now if location of alphabet is already filled then the next positioning of alphabet should be immediate left of present place. Thus, shade dispersion is done via DS arrangement. The logical riddle of DS is used as reconfiguration technique in this thesis. The flowchart is shown in figure 4.18.

a_{11}	a_{12}	a_{13}	a_{14}	a_{15}
b_{21}	b_{22}	b_{23}	b_{24}	b_{25}
c_{31}	c_{32}	c_{33}	c_{34}	c_{35}
d_{41}	d_{42}	d_{43}	d_{44}	d_{45}
e_{51}	e_{52}	e_{53}	e_{54}	e_{55}

Figure 4.16 Alphabetical 5x5 Matrix

c_{31}	e_{54}	b_{22}	d_{41}	a_{13}
a_{14}	c_{32}	e_{55}	b_{23}	d_{42}
d_{43}	a_{15}	c_{33}	e_{51}	b_{24}
b_{25}	d_{44}	a_{11}	c_{34}	e_{52}
e_{53}	b_{21}	d_{45}	a_{12}	c_{35}

Figure 4.17 DS Puzzle Reconfigured Matrix

Using DS puzzle, solar PV system can be reconfigured for obtaining MPP under any type of shading. The first integer and second integer of every panel presents row and column location respectively. To determine the impact of this technique, a 5 × 5 TCT matrix is reconfigured by chasing dominance square pattern and it is shown in figure 4.19. By implementing this puzzle, shade dispersed is achieved and it is in figure 4.20.

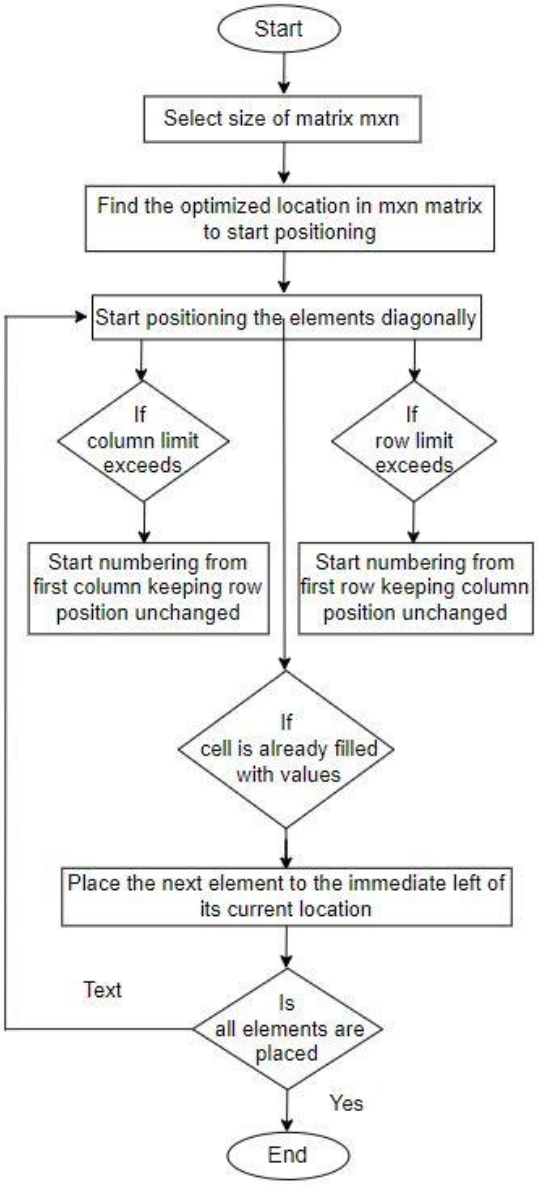

Figure 4.18 Dominance Square Flowchart

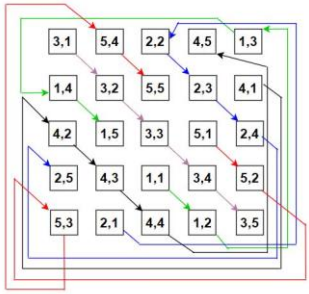

Figure 4.19 Reconfiguring Process

3,1	5,4	2,2	4,5	1,3
1,4	3,2	5,5	2,3	4,1
4,2	1,5	3,3	5,1	2,4
2,5	4,3	1,1	3,4	5,2
5,3	2,1	4,4	1,2	3,5

Figure 4.20 Dominance Square Pattern

4.3.5 Latin Square (LS): Figure 4.21 contains the novel method of LS riddle-based topology, where the locations of panels are rearranged as per revised TCT, without altering the electrical connections. The first integer and second integer of every panel presents row and column location respectively. It is an old riddle in which integers are placed in a specific row and column. Also, every symbol occurs once in every row or column. This has a property containing greater dispersion of shade via reconfiguration at distinct shading scenarios.

1,1	5,2	4,3	3,4	2,5
2,1	1,2	5,3	4,4	3,5
3,1	2,2	1,3	5,4	4,5
4,1	3,2	2,3	1,4	5,5
5,1	4,2	3,3	2,4	1,5

Figure 4.21 Latin Square Pattern

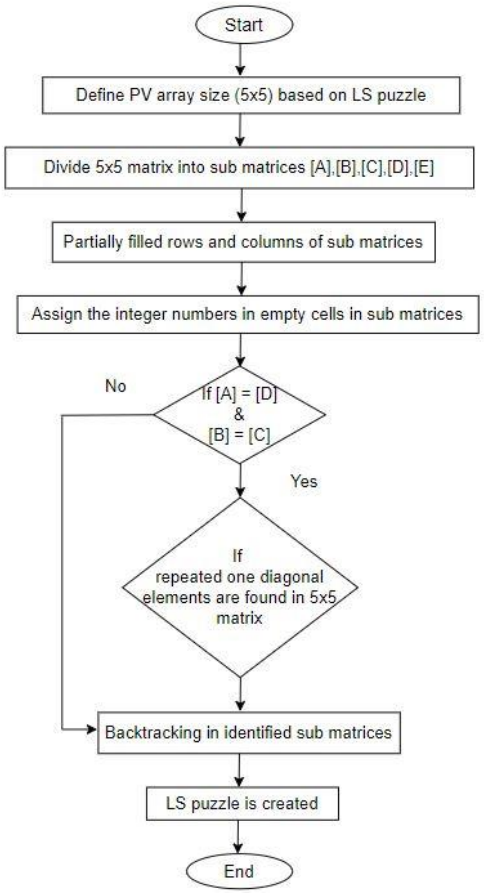

Figure 4.22 Latin Square Flowchart

4.3.6 Odd/Even (OE) structure: The parameters that are used for determining effective performance of an array are maximum power, power losses and fill factor. These features are determined for updated SuDoKu based on TCT configuration. An extensive comparison is followed under shadowing conditions and noticed that the revised SuDoKu method increases the GMPP by 26.9%, 30.3%, 30.8%, 16.8%, 4.2%, and 6.3% as compared to conventional configurations and SuDoKu method of an array [62]. The dispersion of shading scenario decreases the effect on the performance of PV system. For obtaining good amount of shade dispersion, Odd/Even methodology is considered.

The presented technique is separated in two stages. The first part includes the way in which panels are connected. The connections are identical as in case of TCT configuration. The second part contains the steps used for locating the panels.

Let's consider matrix as p by q, i.e., there are p rows and q columns. Every module has a unique identity defined as M ij, where i = 1,2,3…p and j = 1,2,3…q indicates elements of row and column respectively.

A 5x5 matrix is chosen for evaluation of Odd/Even method. The panels in presented method are relocated such that odd panels rows and odd panels column are located first followed by odd panels rows and even panels column. Figure 4.23 shows the Odd/Even pattern.

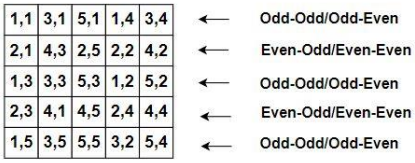

Figure 4.23 Odd/Even Pattern

4.3.7 Skyscraper puzzle: To evaluate the procedure of skyscraper puzzle, a 5x5 matrix considers height of rearranged blocks. It is important that height based visible blocks should be highlighted on every side of an array. For placing blocks in the 5x5 matrix, rows are represented by subscript m and columns are represented by subscript n. Where, m provides total rows and n provides total columns.

This riddle is used to calculate the heights of a blocks of buildings. The visible blocks are identified by numbers at the edges of the block. Taller grids restrict the view of shorter grids behind them. Every row and column must attain exactly 1 building of each height.

Step 1: Evaluate the dimensions of the skyscraper riddle and the total grid heights accessible. In few cases, these are identical and the whole grid is loaded with skyscrapers. While for others, voids may occur. The difference between rows length and total heights is used to determine number of voids in every row. For instance, in figure 4.24, five building heights are there and in 5x5 matrix there is one void in every row and column.

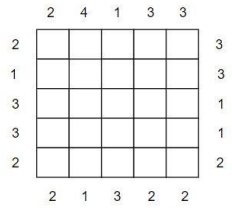

Figure 4.24 Step 1 for Creating Skyscraper Puzzle

Step2: Notice the boundaries. The highest building will restrict all in that particular row or particular column and thus unable to be located next to any number except one. If digit one occurs repeatedly in a particular row, then one among them should be void. As in this instance, there are four building heights and every row and column. The place where void has to be located provides one step forward towards the solution. Figure 4.25 shows the implementation of step 2.

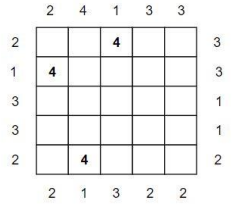

Figure 4.25. Step 2 for Creating Skyscraper Puzzle

Step3: Now other places have to be found which includes building and then mark the grids as given in figure 4.26. If a building is of greatest height, then there should be equal number of buildings between it and each boundary as total buildings seen from that boundary.

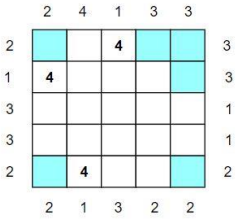

Figure 4.26 Step 3 for Creating Skyscraper Puzzle

Step 4: Determine rows and columns from which building order can be calculated. If the condition occurs such that total seen buildings equals number of building heights, then they should be in enhancing height. If the places of all voids in that particular row or column are also specified, then that particular row can be completely solved. Figure 4.27 shows creation of step 4.

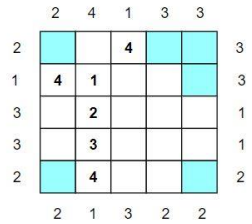

Figure 4.27 Step 4 for Creating Skyscraper Puzzle

Step 5: Now some of the rows and columns are already filled and remaining voids have to be filled by missing numbers. For instance, the 2nd row may be either 4123 or 4132, but 4132 has three buildings seen from the right. Thus, the right boundary should be at height 2, as it can not be empty. Step 5 creation is given in figure 4.28.

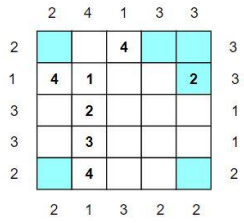

Figure 4.28 Step 5 for Creating Skyscraper Puzzle

Step 6: The other higher buildings should be placed around the boundaries. For instance, as maximum height is 4, a 3 may be placed on a boundary where the total seen buildings is 2. Figure 4.29 shows the implementation of step 6.

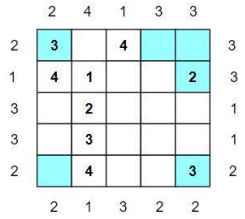

Figure 4.29 Step 6 for Creating Skyscraper Puzzle

Step 7: By locating 3 & 4, the upper most row should be 3421 in which 3 buildings are seen from the right and 1st column should be 3412 in which 2 buildings are seen from below. Mark the rows and columns in which constraints are matched. Figure 4.30 presents implementation of step 7.

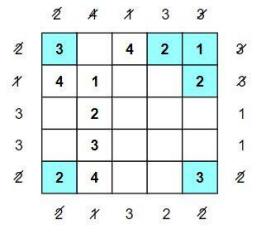

Figure 4.30 Step 7 for Creating Skyscraper Puzzle

Step 8: Notice the mostly filled and use LS constraint to locate rest of the buildings of same height. Figure 4.31 shows creation of step 8.

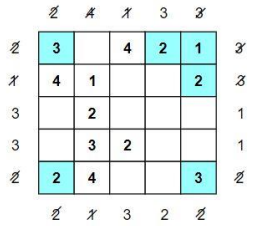

Figure 4.31 Step 8 for Creating Skyscraper Puzzle

Step 9: Find the elements to be filled in voids. For instance, the 4th row has 2 buildings seen from the left. Thus, the voids of 3rd and 4th rows can be calculated. The step 9 is shown by figure 4.32.

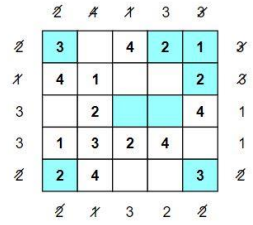

Figure 4.32 Step 9 for Creating Skyscraper Puzzle

Step 10: The total seen buildings from bottom can be used for finding rest of the elements. Figure 4.33 shows the processing of step 10.

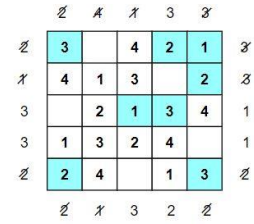

Figure 4.33 Step 10 for Creating Skyscraper Puzzle

The final skyscraper puzzle is created by following 10 steps and shown by figure 4.34.

3	5	4	2	1
4	1	3	5	2
5	2	1	3	4
1	3	2	4	5
2	4	5	1	3

Figure 4.34 Skyscraper Puzzle

4.3.8 Competence Square (CS): The CS opts a logical digit placement which places letters/digits for m × n matrix. In this, placing numbers indicates locating alphabets and numbers in a specified sequence. The 5x5 matrix can be revised via CS puzzle by using following rules.

1: Firstly, the module located at a11 is transferred to a22. This can be selected randomly all over an array according to shading scenario.

2: While going through placing the alphabets, if limit of a row m>5 then start filling the elements from next row with first column.

3: Similarly, if limit of a column n>5, then start filling the elements from next row with first column.

4: If in case, a place is already occupied then locate the alphabet in the same row at the position which is near to it.

The alphabetical matrix which is created by following the rules is shown in figure 4.35 and the complete competence matrix is given by figure 4.36.

a_{11}	a_{12}	a_{13}	a_{14}	a_{15}
b_{21}	b_{22}	b_{23}	b_{24}	b_{25}
c_{31}	c_{32}	c_{33}	c_{34}	c_{35}
d_{41}	d_{42}	d_{43}	d_{44}	d_{45}
e_{51}	e_{52}	e_{53}	e_{54}	e_{55}

Figure 4.35 Alphabetical Matrix

2,5	3,5	4,5	5,5	1,5
5,1	1,1	2,1	3,1	4,1
3,2	4,2	5,2	1,2	2,2
1,3	2,3	3,3	4,3	5,3
4,4	5,4	1,4	2,4	3,4

Figure 4.36 Competence Square Pattern

4.3.9 SuDoKu: This provides method based on logic but it is difficult to implement. A 5× 5 matrix is taken for SuDoKu TCT topology in which 1st number indicates row and 2nd number indicates column as shown in figure 4.37. As far as performance is considered, SuDoKu is better even at shading transitions. The rearrangement of panels is limited by enhancement of wires cost.

5,1	4,2	3,3	1,4	2,5
2,1	1,2	5,3	3,4	4,5
1,1	3,2	2,3	4,4	5,5
4,1	2,2	1,3	5,4	3,5
3,1	5,2	4,3	2,4	1,5

Figure 4.37 SuDoKu Pattern

4.3.10 Magic Square (MS): The MS is a special pattern such that summing of elements of every row, every column and diagonals provides identical number known as magic number. The 1st integer indicates row and 2nd integer indicates column. In this topology, connections are unaltered and modules get reconfigured as given in figure 4.38. MS performs well with respect to other topologies at different shading scenarios but because of reconfiguration, its implementation is a tough and thus its cost enhances. The equations (37)-(61) explains elements of this topology. The steps are as follows:

1. The data of 1st column is determined by equations (37)-(41).

$$\text{Row1} = 1,1 \quad (37)$$

$$\text{Row2} = 2,1 \quad (38)$$

$$\text{Row3} = 3,1 \quad (39)$$

$$\text{Row4} = 4,1 \quad (40)$$

$$\text{Row5} = 5,1 \quad (41)$$

2. The data of 2nd column is determined by equations (42)-(46)

Row1 = 4,2 (42)

Row2 = 5,2 (43)

Row3 = 1,2 (44)

Row4 = 2,2 (45)

Row5 = 3,2 (46)

3. The data of 3rd column is determined by equations (47)-(51)

Row1 = 2,3 (47)

Row2 = 3,3 (48)

Row3 = 4,3 (49)

Row4 = 5,3 (50)

Row5 = 1,3 (51)

4. The data of 4th column is determined by equations (52)-(56)

Row1 = 5,4 (52)

Row2 = 1,4 (53)

Row3 = 2,4 (54)

Row4 = 3,4 (55)

Row5 = 4,4 (56)

5. The data of 5th column is determined by equations (57)-(61)

Row1 = 3,5 (57)

Row2 = 4,5 (58)

Row3 = 5,5 (59)

Row4 = 1,5 (60)

Row5 = 2,5 (61)

1,1	4,2	2,3	5,4	3,5
2,1	5,2	3,3	1,4	4,5
3,1	1,2	4,3	2,4	5,5
4,1	2,2	5,3	3,4	1,5
5,1	3,2	1,3	4,4	2,5

Figure 4.38 MS Puzzle

CHAPTER 5

ANALYSIS OF CONFIGURATIONS AT VARIOUS SHADING CONDITIONS

5.1 Shading Patterns

The solar systems are implemented in many applications such as solar farms, standalone solar system, building integrated PV systems and so on. The improper illumination leads in shading. The shading may be caused due to high rise buildings, big trees, moving clouds, moving planes etc. Even a small portion of shade can negatively affect the efficiency of PV system. These shading losses occurs due to obstacle between panel and sun beam. As a module gets shaded, it starting acts as a load instead of contributing as a source. The whole power produced by unshaded panels is dissipated in the shaded panel which leads to high losses. This is named as shading loss. The distinct configurations have gone through five shading scenarios for evaluation. These scenarios are based on total shaded columns and total shaded modules per column. The types of shades are: Long Narrow (LN), Short Narrow (SN), Long Wide (LW), Short Wide (SW) as shown in figure 5.1 (a). Diagonal pattern is also considered for 5x5 array.

5.1.1 Short Narrow Analysis: A few variations in irradiance are implemented in SN shading case. Also, irradiance selected in this case is narrow, therefore its effect is less and its GMPP is in narrow bandwidth. The short narrow case is represented in figure 5.1 (b).

5.1.2 Short Wide Analysis: A wide shade case is implemented which shaded last 2 rows of PV system. The short wide scenario in an array is shown in figure 5.1 (c). The 1st three rows constantly receive 1000 W/m^2 and the rest 2 rows receives 300 W/m^2 in first two columns, 600 W/m^2 in third and fourth column and 800 W/m^2 in fifth column.

5.1.3 Long Narrow Analysis: The shading of last two columns matches the case of long narrow of PV system as in figure 5.1 (d). In this case, the panels of 1st three columns and

1st two rows receive 1000 W/m^2 and the remaining panels receive 300 W/m^2, 600 W/m^2 and 800 W/m^2.

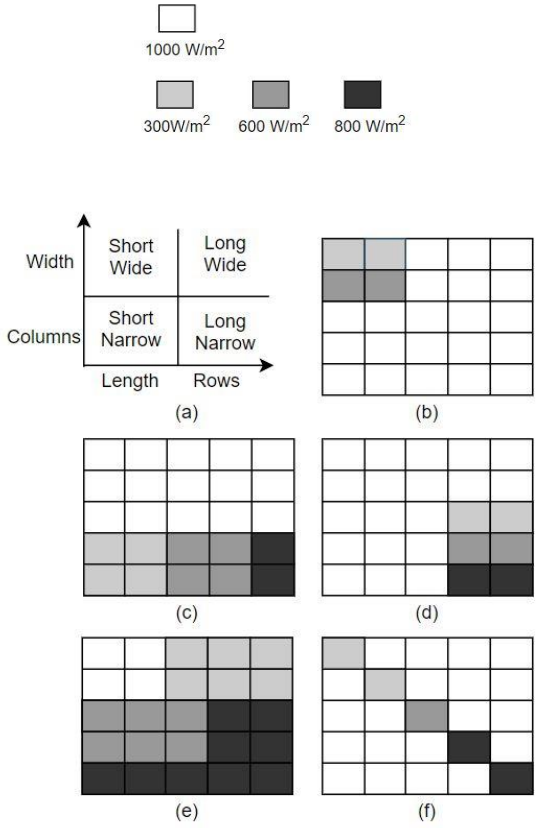

Figure 5.1 (a) Shading Patterns (b) SN (c) SW (d) LN (e) LW (f) Diagonal

5.1.4 Long Wide Analysis: A wide variations in irradiance are implemented in long wide case as in figure 5.1 (e). The 1st two rows and 1st two columns receive 1000 W/m^2 and remaining modules receive 300 W/m^2, 600 W/m^2 and 800 W/m^2.

5.1.5 Diagonal Analysis: A diagonal shade shown in figure 5.1 (f) is formed with distinct irradiations. In this, only diagonal elements receive shading of 300 W/m^2, 600 W/m^2 and 800 W/m^2.

5.2 Analysis of Different Configurations

5.2.1 Series Parallel (SP): Many peaks occurred in case of series connection while single peak occurs in parallel connection at shading conditions. SP is widely used topology as it

is simple to implement. The whole power is improved but its performance is lacking under shadowing conditions. The SP pattern defining various shades is shown by figure 5.2.

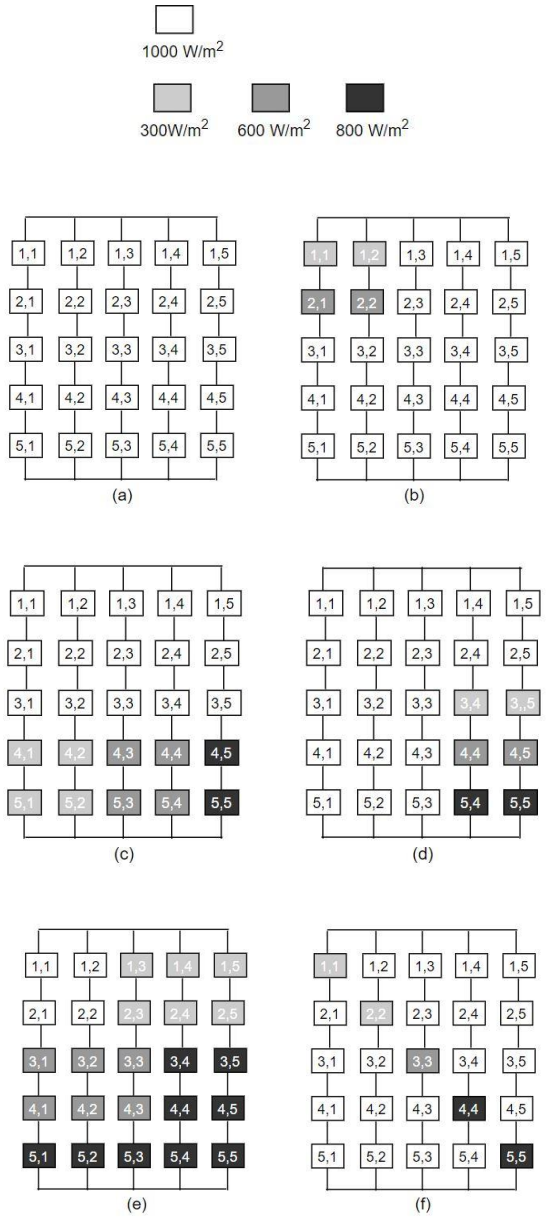

Figure 5.2 (a) SP Connection (b) SN (c) SW (d) LN (e) LW (f) Diagonal

5.2.2 Total Cross Tied (TCT): TCT connections are difficult to apply with respect to SP. It includes rows and columns which are crossly connected. TCT technique overcomes problems of SP configuration under shading scenarios but it goes through a disadvantage in case of total leading greatest cable losses. TCT is divided into two categories: Bridge

Link and Honey Comb. The TCT configurations defining various shades is shown by figure 5.3.

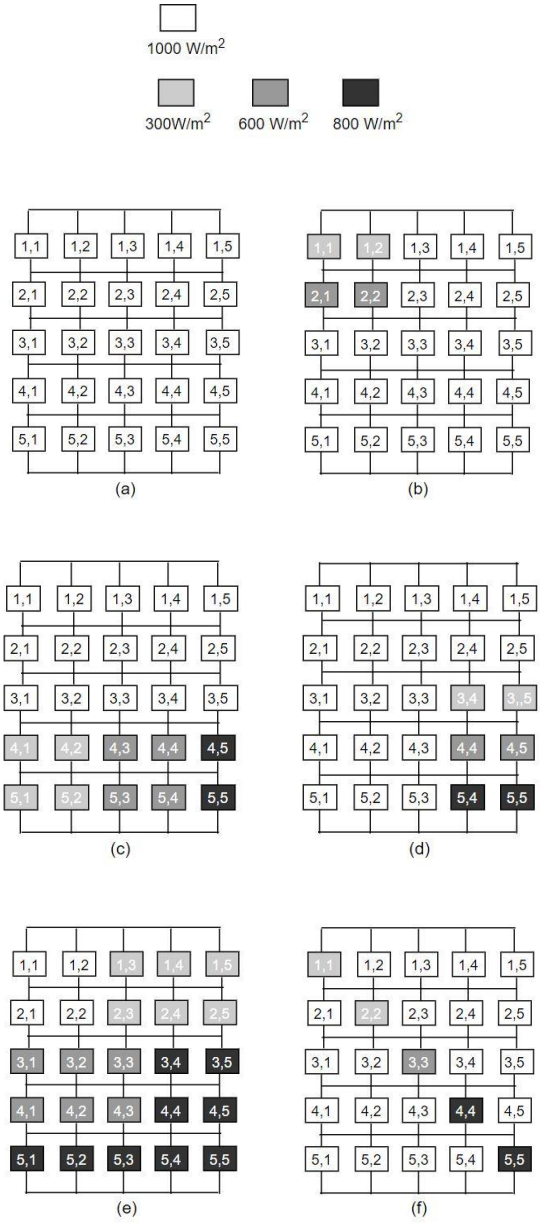

Figure 5.3 (a) TCT Configuration (b) SN (c) SW (d) LN (e) LW (f) Diagonal

5.2.2.1 Bridge Linked (BL): BL is named so as it is based on bridge rectifier structure as in figure 5.4. It is one of the classifications of TCT which has overcome the drawback of a greater number of ties. It also has a merit of reduction in time of wire furnishing. Its drawback is that it severely affects total voltage and current under shadowing conditions.

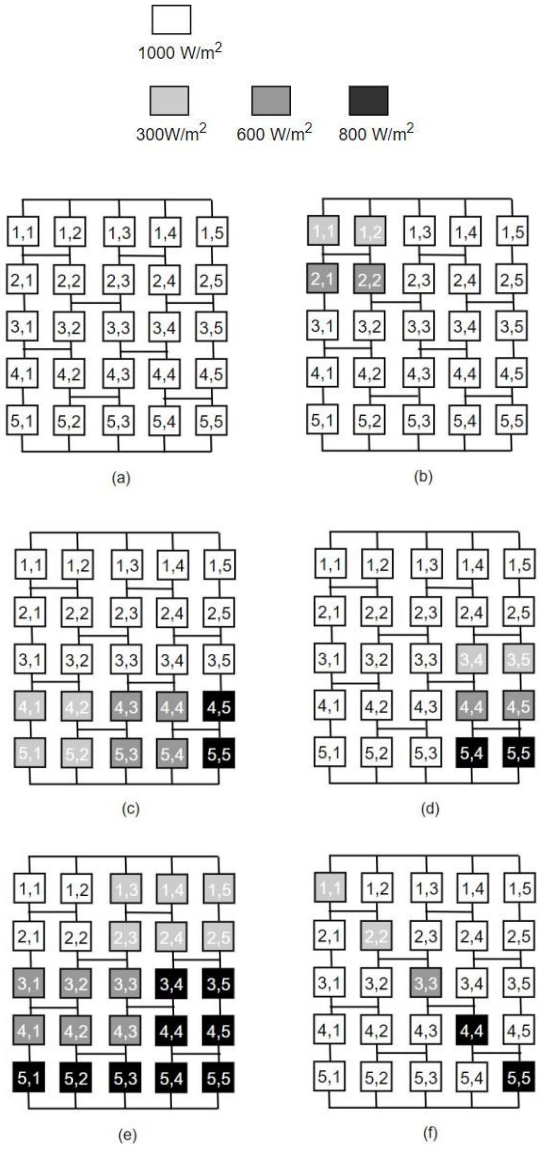

Figure 5.4 (a) BL Configuration (b) SN (c) SW (d) LN (e) LW (f) Diagonal

5.2.2.2 Honey Comb (HC): The HC is based on honeycomb structure as in figure 5.5. It has an advantage of reduction in output power losses and a disadvantage of unable to reduce power losses under all shades.

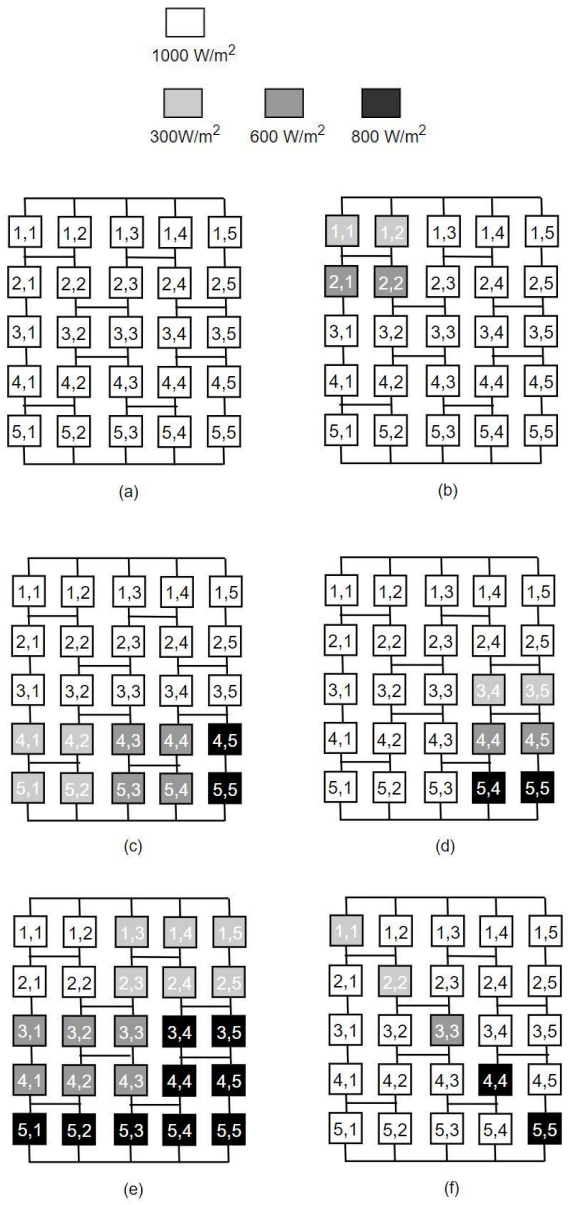

Figure 5.5 (a) HC Configuration (b) SN (c) SW (d) LN (e) LW (f) Diagonal

5.2.3 Ladder: The ladder pattern can defeat the demerits of bridge link and series parallel connections. In this, the panels of first and second column are joined in parallel, and after those rows are connected in series as in figure 5.6. The final structure seems as a ladder, thus named ladder configuration. The total current of PV system is addition of all module currents. This arrangement does not have any modules joined in series while rows are concatenated in series. Thus, the mismatch loss is lower than the bridge link, and series parallel and greater than TCT, honey comb and other hybrid topologies.

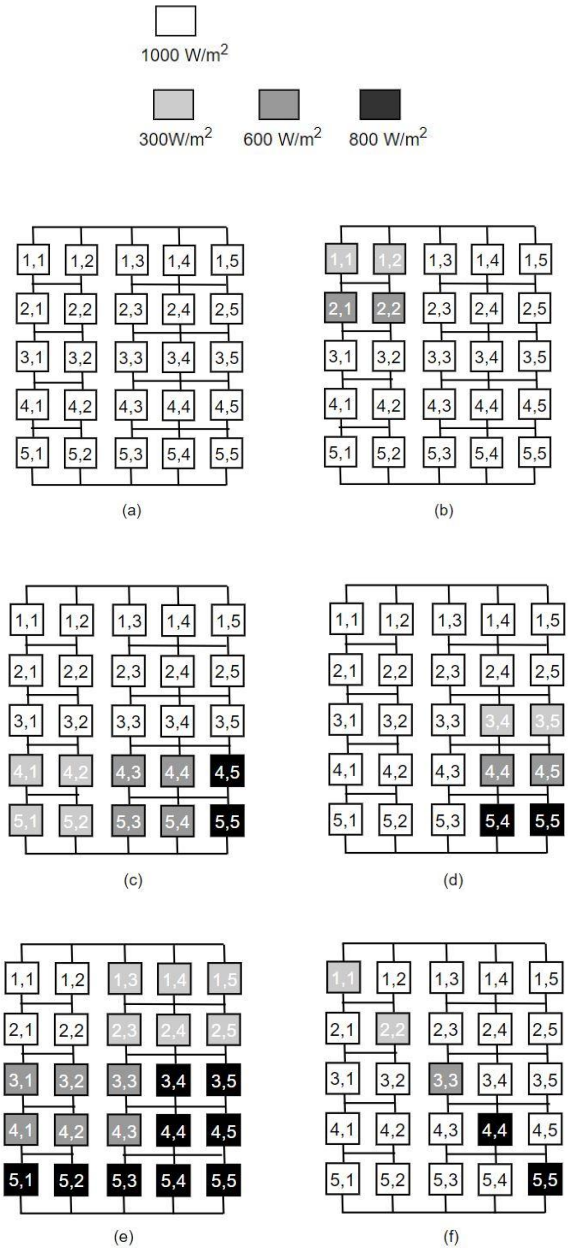

Figure 5.6 (a) Ladder Configuration (b) SN (c) SW (d) LN (e) LW (f) Diagonal

5.2.4 PRM-FEC: An advantage of shade spreading is taken care in this method. The spreading restricts large amount of shade in a single row or column. As far as connections are concerned, they are matched with the connections of TCT but panels are relocated to a new position. The shading panels along with shading scenarios that are different from TCT and SP are shown in figure 5.7. A problem that occurs in this method is complexity in implementation because of panels relocation which finally enhances the price of wires.

This method uses algorithm based on odd row. To obtain the desired results, repetition of row elements or column elements are not considered in this method.

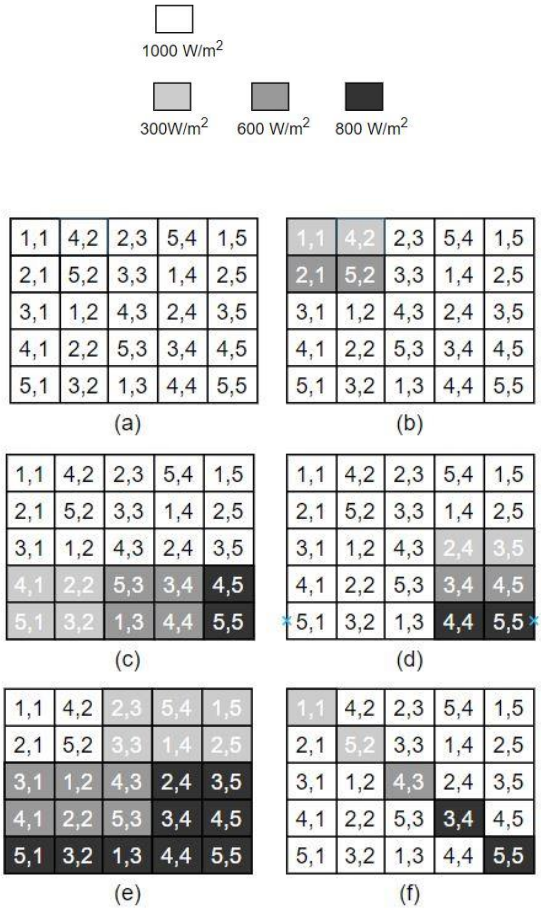

Figure 5.7 (a) PRM-FEC Configuration (b) SN (c) SW (d) LN (e) LW (f) Diagonal

5.2.5 Futoshiki: This is a logical puzzle which can be solved till 9x9 matrix. The comparing signs are used to calculate the elements of futoshiki. For obtaining the elements at primary stage, extract the digits using symbols in futoshiki puzzle. A 5x5 matrix is taken as in figure 5.8 so a single sign of greater following next cell, then the highest cell should be 2,3,4,5 and lowest cell should be 1,2,3,4. The condition a>b>c is essential for obtaining the elements of puzzle. For example, if a is at 3 then c must not be > 3. The general rules of SuDoKu are also helpful in futoshiki pattern.

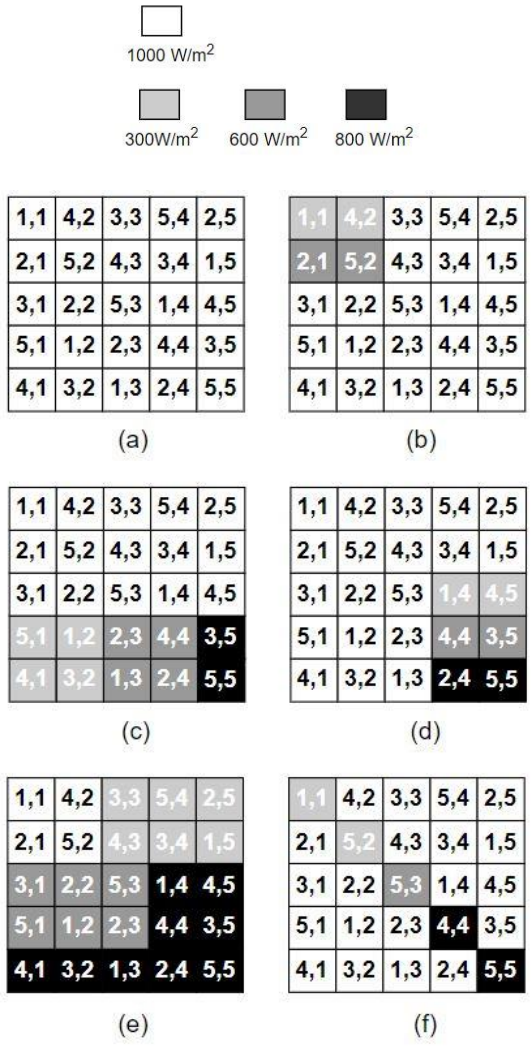

Figure 5.8 (a) Futoshiki Configuration (b) SN (c) SW (d) LN (e) LW (f) Diagonal

5.2.6 Dominance Square: This method goes through dominant square pattern for placing the digits in the matrix. Dominance square is a logical puzzle that arranges letters and digits in sequence. The placement of digits/alphabet in this method shown in figure 5.9.

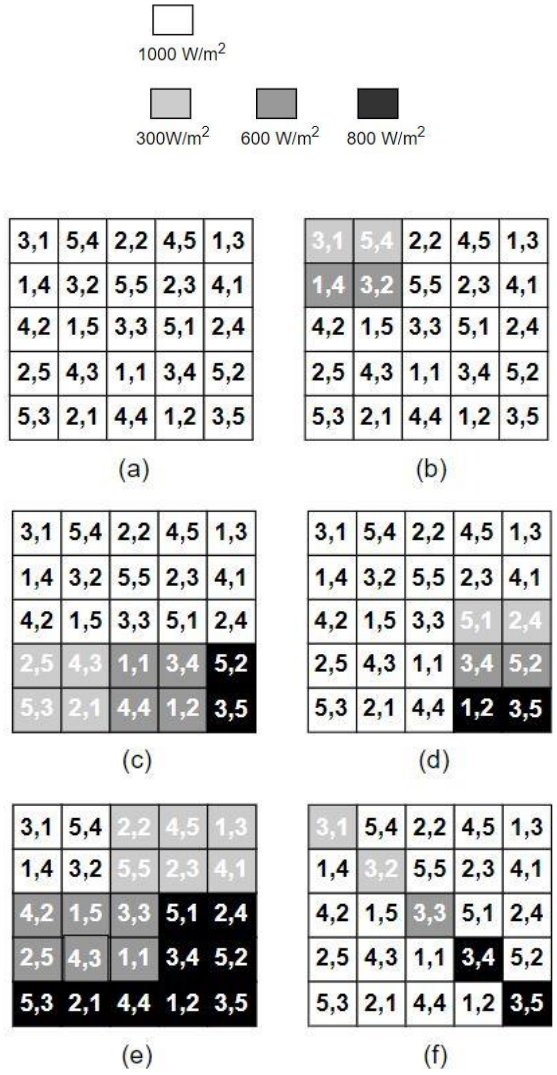

Figure 5.9 (a) DS Configuration (b) SN (c) SW (d) LN (e) LW (f) Diagonal

5.2.7 Latin Square: Figure 5.10 contains the novel method of LS riddle-based topology, where the locations of panels are rearranged as per revised TCT, without altering the electrical connections. The first integer and second integer of every panel presents row and column location respectively. It is an old riddle in which integers are placed in a specific row and column. Also, every symbol occurs once in every row or column. This has a property containing greater dispersion of shade via reconfiguration at distinct shading scenarios.

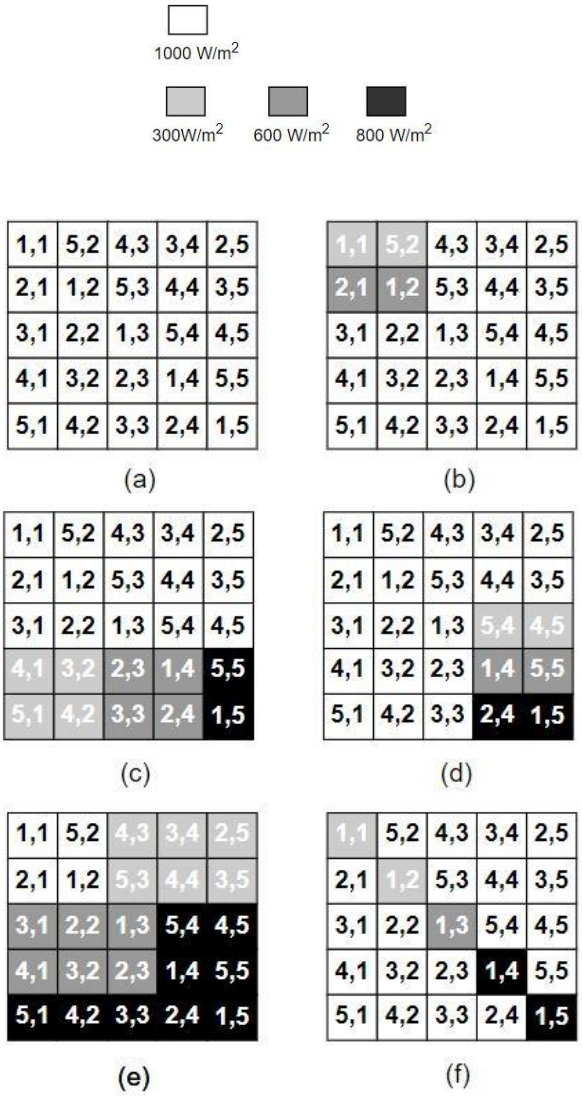

Figure 5.10 (a) LS Configuration (b) SN (c) SW (d) LN (e) LW (f) Diagonal

5.2.8 Odd/Even (OE) structure: The presented technique is separated in two stages as in figure 5.11. The first part includes the way in which panels are connected. The connections are identical as in case of TCT configuration. The second part contains the steps used for locating the panels.

Let's consider matrix as p by q, i.e., there are p rows and q columns. Every module has a unique identity defined as M ij, where i = 1,2,3…p and j = 1,2,3…q indicates elements of row and column respectively.

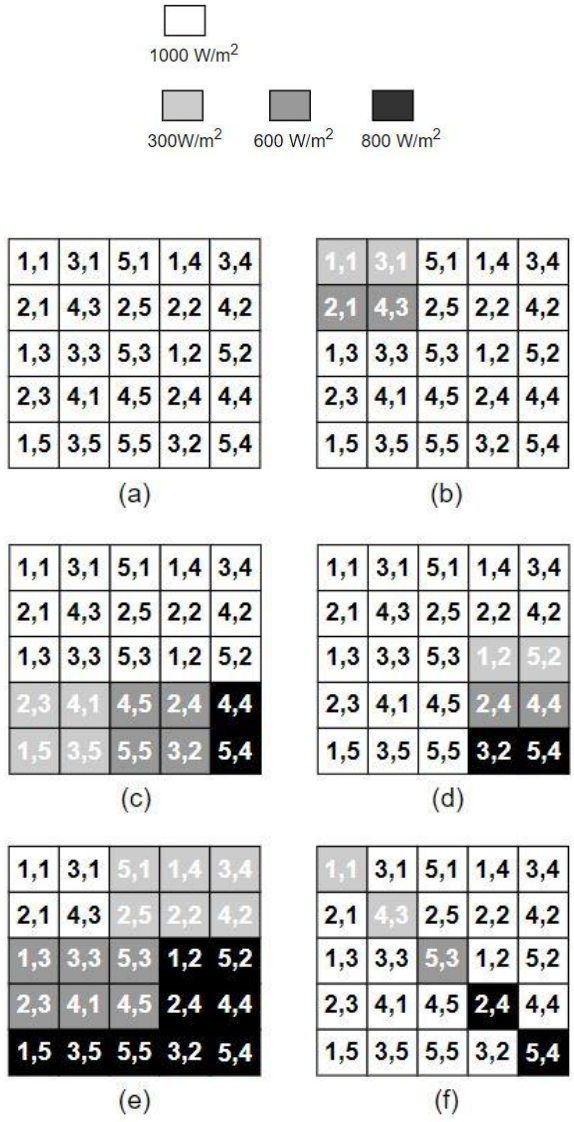

Figure 5.11 (a) Odd Even Configuration (b) SN (c) SW (d) LN (e) LW (f) Diagonal

5.2.9 Skyscraper: To evaluate the procedure of skyscraper puzzle, a 5x5 matrix considers height of rearranged blocks as in figure 5.12. It is important that height based visible blocks should be highlighted on every side of an array. For placing blocks in the 5x5 matrix, rows are represented by subscript m and columns are represented by subscript n. Where, m provides total rows and n provides total columns.

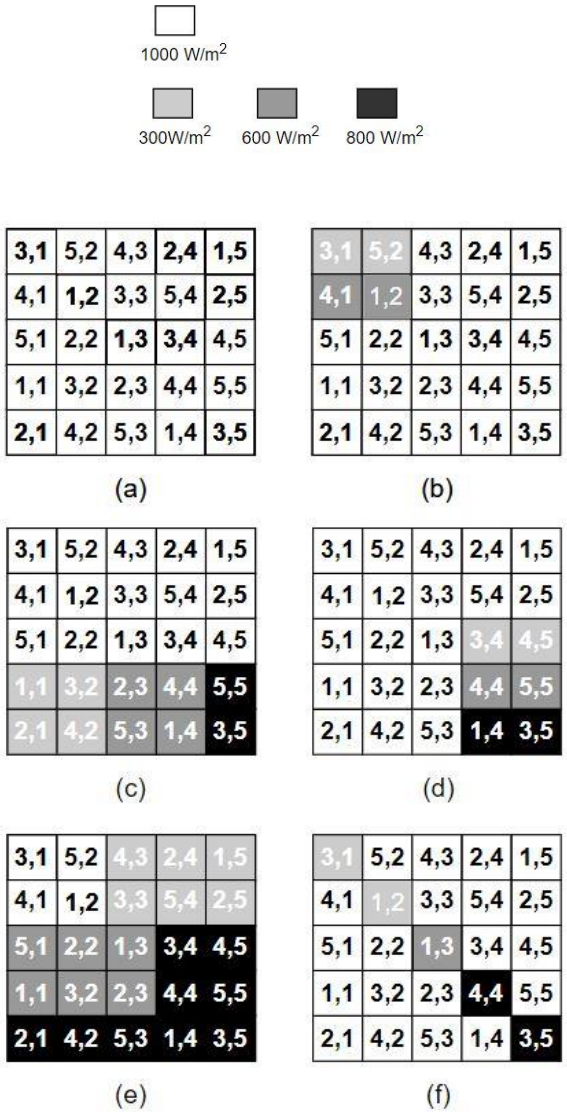

Figure 5.12 (a) Skyscraper Configuration (b) SN (c) SW (d) LN (e) LW (f) Diagonal

5.2.10 Competence Square: The CS opts a logical digit placement which places letters/digits for m × n matrix. In this, placing numbers indicates locating alphabets and numbers in a specified sequence as in figure 5.13.

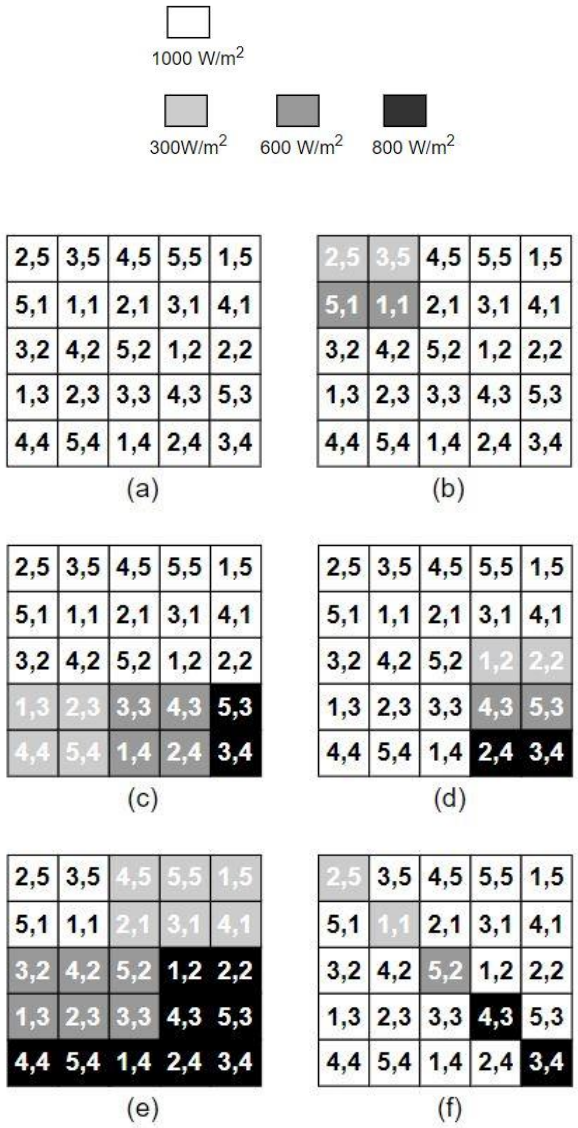

Figure 5.13 (a) CS Configuration (b) SN (c) SW (d) LN (e) LW (f) Diagonal

5.11 SuDoKu: This provides method based on logic but it is complicated to implement. A 5 × 5 matrix is taken for SuDoKu TCT topology in which 1st number indicates row and 2nd number indicates column as shown in figure 5.14. As far as performance is considered, SuDoKu is better even at shading transitions. The rearrangement of panels is limited by enhancement of wires cost.

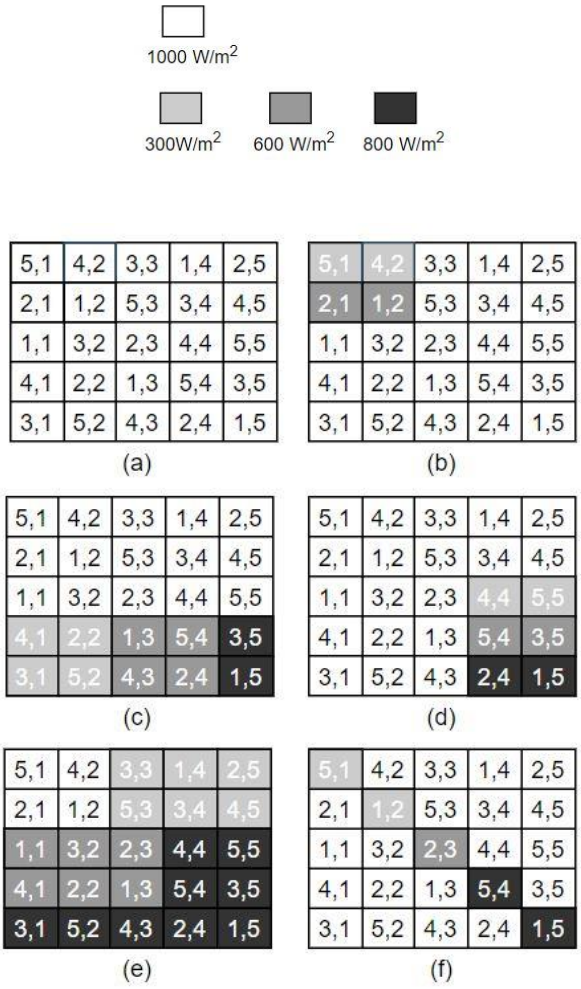

Figure 5.14 (a) SuDoKu Configuration (b) SN (c) SW (d) LN (e) LW (f) Diagonal

5.2.12 MS: The MS is a special pattern such that summing of elements of every row, every column and diagonals provides identical number known as magic number. The 1st integer indicates row and 2nd integer indicates column. In this topology, connections are unaltered and modules get reconfigured as given in figure 5.15. MS performs well with respect to other topologies at different shading scenarios but because of reconfiguration, its implementation is a tough and thus its cost enhances.

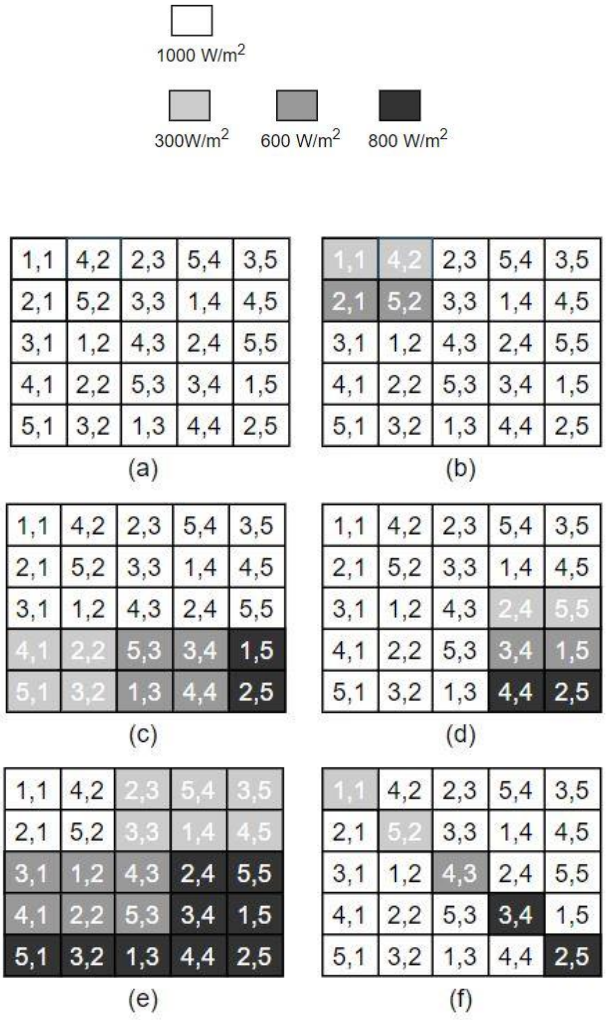

Figure 5.15 (a) MS Configuration (b) SN (c) SW (d) LN (e) LW (f) Diagonal

5.3 Simulation results

Distinct shading scenarios are applied on various topologies for extracting their performance. In this thesis, unshaded modules receive 1000W/m^2 irradiation while shaded modules receives 600 W/m^2 irradiation. The module current and power varies with the variation in irradiance which is described in table 5.1 – 5.5.

Table 5.1 Evaluation of Various Topologies Based on Short Narrow Pattern

Configurations	I(Amp.)	V(Volt)	P(Watt)
SP, TCT, BL, HC, LD	$I_{row1} = 3.6\ I_m$	V_m	$3.6\ V_m\ I_m$
	$I_{row2} = 4.2\ I_m$	$2V_m$	$8.4\ V_m\ I_m$
	$I_{row3} = 5.0\ I_m$	$3V_m$	$15.0\ V_m\ I_m$
	$I_{row4} = 5.0\ I_m$	$4V_m$	$20.0\ V_m\ I_m$
	$I_{row5} = 5.0\ I_m$	$5V_m$	$25.0\ V_m\ I_m$
PRM-FEC	$I_{row1} = 4.3\ I_m$	V_m	$4.3\ V_m\ I_m$
	$I_{row2} = 4.6\ I_m$	$2V_m$	$9.2\ V_m\ I_m$
	$I_{row3} = 5.0\ I_m$	$3V_m$	$15.0\ V_m\ I_m$
	$I_{row4} = 4.3\ I_m$	$4V_m$	$17.2\ V_m\ I_m$
	$I_{row5} = 4.6\ I_m$	$5V_m$	$23.0\ V_m\ I_m$
Futoshiki	$I_{row1} = 4.3\ I_m$	V_m	$4.3\ V_m\ I_m$
	$I_{row2} = 4.6\ I_m$	$2V_m$	$9.2\ V_m\ I_m$
	$I_{row3} = 5.0\ I_m$	$3V_m$	$15.0\ V_m\ I_m$
	$I_{row4} = 4.3\ I_m$	$4V_m$	$17.2\ V_m\ I_m$
	$I_{row5} = 4.6\ I_m$	$5V_m$	$23.0\ V_m\ I_m$
DS	$I_{row1} = 4.6\ I_m$	V_m	$4.6\ V_m\ I_m$
	$I_{row2} = 5.0\ I_m$	$2V_m$	$10.0\ V_m\ I_m$
	$I_{row3} = 3.9\ I_m$	$3V_m$	$11.7\ V_m\ I_m$
	$I_{row4} = 5.0\ I_m$	$4V_m$	$20.0\ V_m\ I_m$
	$I_{row5} = 4.3\ I_m$	$5V_m$	$21.5\ V_m\ I_m$
LS	$I_{row1} = 3.9\ I_m$	V_m	$3.9\ V_m\ I_m$
	$I_{row2} = 4.6\ I_m$	$2V_m$	$9.2\ V_m\ I_m$
	$I_{row3} = 5.0\ I_m$	$3V_m$	$15.0\ V_m\ I_m$
	$I_{row4} = 5.0\ I_m$	$4V_m$	$20.0\ V_m\ I_m$
	$I_{row5} = 4.3\ I_m$	$5V_m$	$21.5\ V_m\ I_m$

OE	$I_{row1} = 4.3\ I_m$	V_m	$4.3\ V_m\ I_m$
	$I_{row2} = 4.6\ I_m$	$2V_m$	$9.2\ V_m\ I_m$
	$I_{row3} = 4.3\ I_m$	$3V_m$	$12.9\ V_m\ I_m$
	$I_{row4} = 4.6\ I_m$	$4V_m$	$18.4\ V_m\ I_m$
	$I_{row5} = 5.0\ I_m$	$5V_m$	$25.0\ V_m\ I_m$
Skyscraper	$I_{row1} = 4.6\ I_m$	V_m	$4.6\ V_m\ I_m$
	$I_{row2} = 5.0\ I_m$	$2V_m$	$10.0\ V_m\ I_m$
	$I_{row3} = 4.3\ I_m$	$3V_m$	$12.9\ V_m\ I_m$
	$I_{row4} = 4.6\ I_m$	$4V_m$	$18.4\ V_m\ I_m$
	$I_{row5} = 4.3\ I_m$	$5V_m$	$21.5\ V_m\ I_m$
CS	$I_{row1} = 4.6\ I_m$	V_m	$4.6\ V_m\ I_m$
	$I_{row2} = 4.3\ I_m$	$2V_m$	$8.6\ V_m\ I_m$
	$I_{row3} = 4.3\ I_m$	$3V_m$	$12.9\ V_m\ I_m$
	$I_{row4} = 5.0\ I_m$	$4V_m$	$20.0\ V_m\ I_m$
	$I_{row5} = 4.6\ I_m$	$5V_m$	$23.0\ V_m\ I_m$
SuDoKu	$I_{row1} = 4.6\ I_m$	V_m	$4.6\ V_m\ I_m$
	$I_{row2} = 4.6\ I_m$	$2V_m$	$9.2\ V_m\ I_m$
	$I_{row3} = 5.0\ I_m$	$3V_m$	$15.0\ V_m\ I_m$
	$I_{row4} = 4.3\ I_m$	$4V_m$	$17.2\ V_m\ I_m$
	$I_{row5} = 4.3\ I_m$	$5V_m$	$21.5\ V_m\ I_m$
MS	$I_{row1} = 4.3\ I_m$	V_m	$4.3\ V_m\ I_m$
	$I_{row2} = 4.6\ I_m$	$2V_m$	$9.2\ V_m\ I_m$
	$I_{row3} = 5.0\ I_m$	$3V_m$	$15.0\ V_m\ I_m$
	$I_{row4} = 4.3\ I_m$	$4V_m$	$17.2\ V_m\ I_m$
	$I_{row5} = 4.6\ I_m$	$5V_m$	$23.0\ V_m\ I_m$

Table 5.2 Evaluation of Various Topologies Based on Short Wide Pattern

Configurations	I(Amp.)	V(Volt)	P(Watt)
SP, TCT, BL, HC, LD	$I_{row1} = 5.0\ I_m$	V_m	$5.0\ V_m\ I_m$
	$I_{row2} = 5.0\ I_m$	$2V_m$	$10.0\ V_m\ I_m$
	$I_{row3} = 5.0\ I_m$	$3V_m$	$15.0\ V_m\ I_m$
	$I_{row4} = 2.6\ I_m$	$4V_m$	$10.4\ V_m\ I_m$
	$I_{row5} = 2.6\ I_m$	$5V_m$	$13.0\ V_m\ I_m$
PRM-FEC	$I_{row1} = 4.6\ I_m$	V_m	$4.6\ V_m\ I_m$
	$I_{row2} = 4.3\ I_m$	$2V_m$	$8.6\ V_m\ I_m$
	$I_{row3} = 3.9\ I_m$	$3V_m$	$11.7\ V_m\ I_m$
	$I_{row4} = 3.7\ I_m$	$4V_m$	$14.8\ V_m\ I_m$
	$I_{row5} = 3.7\ I_m$	$5V_m$	$18.5\ V_m\ I_m$
Futoshiki	$I_{row1} = 3.9\ I_m$	V_m	$3.9\ V_m\ I_m$
	$I_{row2} = 4.2\ I_m$	$2V_m$	$8.4\ V_m\ I_m$
	$I_{row3} = 4.1\ I_m$	$3V_m$	$12.3\ V_m\ I_m$
	$I_{row4} = 3.9\ I_m$	$4V_m$	$15.6\ V_m\ I_m$
	$I_{row5} = 4.1\ I_m$	$5V_m$	$20.5\ V_m\ I_m$
DS	$I_{row1} = 4.2\ I_m$	V_m	$4.2\ V_m\ I_m$
	$I_{row2} = 3.6\ I_m$	$2V_m$	$7.2\ V_m\ I_m$
	$I_{row3} = 4.4\ I_m$	$3V_m$	$13.2\ V_m\ I_m$
	$I_{row4} = 3.9\ I_m$	$4V_m$	$15.6\ V_m\ I_m$
	$I_{row5} = 4.1\ I_m$	$5V_m$	$20.5\ V_m\ I_m$
LS	$I_{row1} = 4.4\ I_m$	V_m	$4.4\ V_m\ I_m$
	$I_{row2} = 4.2\ I_m$	$2V_m$	$8.4\ V_m\ I_m$
	$I_{row3} = 3.9\ I_m$	$3V_m$	$11.7\ V_m\ I_m$

	$I_{row4} = 3.6\ I_m$	$4V_m$	$14.4\ V_m\ I_m$
	$I_{row5} = 4.1\ I_m$	$5V_m$	$20.5\ V_m\ I_m$
OE	$I_{row1} = 4.3\ I_m$	V_m	$4.3\ V_m\ I_m$
	$I_{row2} = 3.9\ I_m$	$2V_m$	$7.8\ V_m\ I_m$
	$I_{row3} = 3.9\ I_m$	$3V_m$	$11.7\ V_m\ I_m$
	$I_{row4} = 3.7\ I_m$	$4V_m$	$14.8\ V_m\ I_m$
	$I_{row5} = 4.4\ I_m$	$5V_m$	$22.0\ V_m\ I_m$
Skyscraper	$I_{row1} = 3.9\ I_m$	V_m	$3.9\ V_m\ I_m$
	$I_{row2} = 3.9\ I_m$	$2V_m$	$7.8\ V_m\ I_m$
	$I_{row3} = 4.1\ I_m$	$3V_m$	$12.3\ V_m\ I_m$
	$I_{row4} = 3.9\ I_m$	$4V_m$	$15.6\ V_m\ I_m$
	$I_{row5} = 4.4\ I_m$	$5V_m$	$22.0\ V_m\ I_m$
CS	$I_{row1} = 3.9\ I_m$	V_m	$3.9\ V_m\ I_m$
	$I_{row2} = 3.9\ I_m$	$2V_m$	$7.8\ V_m\ I_m$
	$I_{row3} = 4.4\ I_m$	$3V_m$	$13.2\ V_m\ I_m$
	$I_{row4} = 3.9\ I_m$	$4V_m$	$15.6\ V_m\ I_m$
	$I_{row5} = 4.1\ I_m$	$5V_m$	$20.5\ V_m\ I_m$
SuDoKu	$I_{row1} = 4.4\ I_m$	V_m	$4.4\ V_m\ I_m$
	$I_{row2} = 3.9\ I_m$	$2V_m$	$7.8\ V_m\ I_m$
	$I_{row3} = 4.1\ I_m$	$3V_m$	$12.3\ V_m\ I_m$
	$I_{row4} = 3.9\ I_m$	$4V_m$	$15.6\ V_m\ I_m$
	$I_{row5} = 3.9\ I_m$	$5V_m$	$19.5\ V_m\ I_m$
MS	$I_{row1} = 4.4\ I_m$	V_m	$4.4\ V_m\ I_m$
	$I_{row2} = 4.1\ I_m$	$2V_m$	$8.2\ V_m\ I_m$
	$I_{row3} = 3.9\ I_m$	$3V_m$	$11.7\ V_m\ I_m$

	$I_{row4} = 3.9\ I_m$	$4V_m$	$15.6\ V_m\ I_m$
	$I_{row5} = 3.9\ I_m$	$5V_m$	$19.5\ V_m\ I_m$

Table 5.3 Evaluation of Various Topologies Based on Long Narrow Pattern

Configurations	I(Amp.)	V(Volt)	P(Watt)
SP, TCT, BL, HC, LD	$I_{row1} = 5.0\ I_m$	V_m	$5.0\ V_m\ I_m$
	$I_{row2} = 5.0\ I_m$	$2V_m$	$10.0\ V_m\ I_m$
	$I_{row3} = 3.6\ I_m$	$3V_m$	$10.8\ V_m\ I_m$
	$I_{row4} = 4.2\ I_m$	$4V_m$	$16.8\ V_m\ I_m$
	$I_{row5} = 4.6\ I_m$	$5V_m$	$23.0\ V_m\ I_m$
PRM-FEC	$I_{row1} = 5.0\ I_m$	V_m	$5.0\ V_m\ I_m$
	$I_{row2} = 4.3\ I_m$	$2V_m$	$8.6\ V_m\ I_m$
	$I_{row3} = 3.9\ I_m$	$3V_m$	$11.7\ V_m\ I_m$
	$I_{row4} = 4.4\ I_m$	$4V_m$	$17.6\ V_m\ I_m$
	$I_{row5} = 4.8\ I_m$	$5V_m$	$24.0\ V_m\ I_m$
Futoshiki	$I_{row1} = 4.3\ I_m$	V_m	$4.3\ V_m\ I_m$
	$I_{row2} = 4.8\ I_m$	$2V_m$	$9.6\ V_m\ I_m$
	$I_{row3} = 4.6\ I_m$	$3V_m$	$13.8\ V_m\ I_m$
	$I_{row4} = 3.9\ I_m$	$4V_m$	$15.6\ V_m\ I_m$
	$I_{row5} = 4.8\ I_m$	$5V_m$	$24.0\ V_m\ I_m$
DS	$I_{row1} = 4.8\ I_m$	V_m	$4.8\ V_m\ I_m$
	$I_{row2} = 4.3\ I_m$	$2V_m$	$8.6\ V_m\ I_m$
	$I_{row3} = 4.4\ I_m$	$3V_m$	$13.2\ V_m\ I_m$
	$I_{row4} = 5.0\ I_m$	$4V_m$	$20.0\ V_m\ I_m$
	$I_{row5} = 3.9\ I_m$	$5V_m$	$19.5\ V_m\ I_m$

LS	$I_{row1} = 4.4\ I_m$	V_m	$4.4\ V_m\ I_m$
	$I_{row2} = 4.8\ I_m$	$2V_m$	$9.6\ V_m\ I_m$
	$I_{row3} = 5.0\ I_m$	$3V_m$	$15.0\ V_m\ I_m$
	$I_{row4} = 4.3\ I_m$	$4V_m$	$17.2\ V_m\ I_m$
	$I_{row5} = 3.9\ I_m$	$5V_m$	$19.5\ V_m\ I_m$
OE	$I_{row1} = 4.3\ I_m$	V_m	$4.3\ V_m\ I_m$
	$I_{row2} = 4.6\ I_m$	$2V_m$	$9.2\ V_m\ I_m$
	$I_{row3} = 4.8\ I_m$	$3V_m$	$14.4\ V_m\ I_m$
	$I_{row4} = 4.6\ I_m$	$4V_m$	$18.4\ V_m\ I_m$
	$I_{row5} = 4.1\ I_m$	$5V_m$	$20.5\ V_m\ I_m$
Skyscraper	$I_{row1} = 4.8\ I_m$	V_m	$4.8\ V_m\ I_m$
	$I_{row2} = 5.0\ I_m$	$2V_m$	$10.0\ V_m\ I_m$
	$I_{row3} = 4.1\ I_m$	$3V_m$	$12.3\ V_m\ I_m$
	$I_{row4} = 3.9\ I_m$	$4V_m$	$15.6\ V_m\ I_m$
	$I_{row5} = 4.6\ I_m$	$5V_m$	$23.0\ V_m\ I_m$
CS	$I_{row1} = 4.3\ I_m$	V_m	$4.3\ V_m\ I_m$
	$I_{row2} = 4.1\ I_m$	$2V_m$	$8.2\ V_m\ I_m$
	$I_{row3} = 4.8\ I_m$	$3V_m$	$14.4\ V_m\ I_m$
	$I_{row4} = 4.6\ I_m$	$4V_m$	$18.4\ V_m\ I_m$
	$I_{row5} = 4.6\ I_m$	$5V_m$	$23.0\ V_m\ I_m$
SuDoKu	$I_{row1} = 4.8\ I_m$	V_m	$4.8\ V_m\ I_m$
	$I_{row2} = 4.8\ I_m$	$2V_m$	$9.6\ V_m\ I_m$
	$I_{row3} = 4.6\ I_m$	$3V_m$	$13.8\ V_m\ I_m$
	$I_{row4} = 4.6\ I_m$	$4V_m$	$18.4\ V_m\ I_m$
	$I_{row5} = 4.6\ I_m$	$5V_m$	$23.0\ V_m\ I_m$
MS	$I_{row1} = 4.6\ I_m$	V_m	$4.6\ V_m\ I_m$
	$I_{row2} = 4.1\ I_m$	$2V_m$	$8.2\ V_m\ I_m$

	$I_{row3} = 4.6\ I_m$	$3V_m$	$13.8\ V_m\ I_m$
	$I_{row4} = 4.8\ I_m$	$4V_m$	$19.2\ V_m\ I_m$
	$I_{row5} = 4.3\ I_m$	$5V_m$	$21.5\ V_m\ I_m$

Table 5.4 Evaluation of Various Topologies Based on Long Wide Pattern

Configurations	I(Amp.)	V(Volt)	P(Watt)
SP, TCT, BL, HC, LD	$I_{row1} = 2.9\ I_m$	V_m	$2.9\ V_m\ I_m$
	$I_{row2} = 2.9\ I_m$	$2V_m$	$5.8\ V_m\ I_m$
	$I_{row3} = 3.4\ I_m$	$3V_m$	$10.2\ V_m\ I_m$
	$I_{row4} = 3.4\ I_m$	$4V_m$	$13.6\ V_m\ I_m$
	$I_{row5} = 4.0\ I_m$	$5V_m$	$20.0\ V_m\ I_m$
PRM-FEC	$I_{row1} = 3.0\ I_m$	V_m	$3.0\ V_m\ I_m$
	$I_{row2} = 3.0\ I_m$	$2V_m$	$6.0\ V_m\ I_m$
	$I_{row3} = 3.3\ I_m$	$3V_m$	$9.9\ V_m\ I_m$
	$I_{row4} = 3.8\ I_m$	$4V_m$	$15.2\ V_m\ I_m$
	$I_{row5} = 3.5\ I_m$	$5V_m$	$17.5\ V_m\ I_m$
Futoshiki	$I_{row1} = 3.5\ I_m$	V_m	$3.5\ V_m\ I_m$
	$I_{row2} = 3.3\ I_m$	$2V_m$	$6.6\ V_m\ I_m$
	$I_{row3} = 2.8\ I_m$	$3V_m$	$8.4\ V_m\ I_m$
	$I_{row4} = 3.7\ I_m$	$4V_m$	$14.8\ V_m\ I_m$
	$I_{row5} = 3.3\ I_m$	$5V_m$	$16.5\ V_m\ I_m$
DS	$I_{row1} = 3.3\ I_m$	V_m	$3.3\ V_m\ I_m$
	$I_{row2} = 2.8\ I_m$	$2V_m$	$5.6\ V_m\ I_m$
	$I_{row3} = 4.2\ I_m$	$3V_m$	$12.6\ V_m\ I_m$
	$I_{row4} = 2.6\ I_m$	$4V_m$	$10.4\ V_m\ I_m$
	$I_{row5} = 3.7\ I_m$	$5V_m$	$18.5\ V_m\ I_m$

LS	$I_{row1} = 4.2\ I_m$	V_m	$4.2\ V_m\ I_m$
	$I_{row2} = 3.3\ I_m$	$2V_m$	$6.6\ V_m\ I_m$
	$I_{row3} = 2.6\ I_m$	$3V_m$	$7.8\ V_m\ I_m$
	$I_{row4} = 2.8\ I_m$	$4V_m$	$11.2\ V_m\ I_m$
	$I_{row5} = 3.7\ I_m$	$5V_m$	$18.5\ V_m\ I_m$
OE	$I_{row1} = 3.5\ I_m$	V_m	$3.5\ V_m\ I_m$
	$I_{row2} = 3.0\ I_m$	$2V_m$	$6.0\ V_m\ I_m$
	$I_{row3} = 3.5\ I_m$	$3V_m$	$10.5\ V_m\ I_m$
	$I_{row4} = 3.3\ I_m$	$4V_m$	$13.2\ V_m\ I_m$
	$I_{row5} = 3.3\ I_m$	$5V_m$	$16.5\ V_m\ I_m$
Skyscraper	$I_{row1} = 3.3\ I_m$	V_m	$3.3\ V_m\ I_m$
	$I_{row2} = 2.6\ I_m$	$2V_m$	$5.2\ V_m\ I_m$
	$I_{row3} = 3.5\ I_m$	$3V_m$	$10.5\ V_m\ I_m$
	$I_{row4} = 3.7\ I_m$	$4V_m$	$14.8\ V_m\ I_m$
	$I_{row5} = 3.5\ I_m$	$5V_m$	$17.5\ V_m\ I_m$
CS	$I_{row1} = 3.5\ I_m$	V_m	$3.5\ V_m\ I_m$
	$I_{row2} = 3.5\ I_m$	$2V_m$	$7.0\ V_m\ I_m$
	$I_{row3} = 3.3\ I_m$	$3V_m$	$9.9\ V_m\ I_m$
	$I_{row4} = 3.0\ I_m$	$4V_m$	$12.0\ V_m\ I_m$
	$I_{row5} = 3.5\ I_m$	$5V_m$	$17.5\ V_m\ I_m$
SuDoKu	$I_{row1} = 3.3\ I_m$	V_m	$3.3\ V_m\ I_m$
	$I_{row2} = 3.3\ I_m$	$2V_m$	$6.6\ V_m\ I_m$
	$I_{row3} = 2.8\ I_m$	$3V_m$	$8.4\ V_m\ I_m$
	$I_{row4} = 3.5\ I_m$	$4V_m$	$14.0\ V_m\ I_m$
	$I_{row5} = 3.7\ I_m$	$5V_m$	$18.5\ V_m\ I_m$

MS	$I_{row1} = 3.5\ I_m$	V_m	$3.5\ V_m\ I_m$
	$I_{row2} = 3.5\ I_m$	$2V_m$	$7.0\ V_m\ I_m$
	$I_{row3} = 2.8\ I_m$	$3V_m$	$8.4\ V_m\ I_m$
	$I_{row4} = 3.3\ I_m$	$4V_m$	$13.2\ V_m\ I_m$
	$I_{row5} = 3.5\ I_m$	$5V_m$	$17.5\ V_m\ I_m$

Table 5.5 Evaluation of Various Topologies Based on Diagonal Pattern

Configurations	I(Amp.)	V(Volt)	P(Watt)
SP, TCT, BL, HC, LD	$I_{row1} = 4.3\ I_m$	V_m	$4.3\ V_m\ I_m$
	$I_{row2} = 4.3\ I_m$	$2V_m$	$8.6\ V_m\ I_m$
	$I_{row3} = 4.6\ I_m$	$3V_m$	$13.8\ V_m\ I_m$
	$I_{row4} = 4.8\ I_m$	$4V_m$	$19.2\ V_m\ I_m$
	$I_{row5} = 4.8\ I_m$	$5V_m$	$24.0\ V_m\ I_m$
PRM-FEC	$I_{row1} = 4.3\ I_m$	V_m	$4.3\ V_m\ I_m$
	$I_{row2} = 5.0\ I_m$	$2V_m$	$10.0\ V_m\ I_m$
	$I_{row3} = 4.8\ I_m$	$3V_m$	$14.4\ V_m\ I_m$
	$I_{row4} = 4.6\ I_m$	$4V_m$	$18.4\ V_m\ I_m$
	$I_{row5} = 4.1\ I_m$	$5V_m$	$20.5\ V_m\ I_m$
Futoshiki	$I_{row1} = 4.3\ I_m$	V_m	$4.3\ V_m\ I_m$
	$I_{row2} = 5.0\ I_m$	$2V_m$	$10.0\ V_m\ I_m$
	$I_{row3} = 5.0\ I_m$	$3V_m$	$15.0\ V_m\ I_m$
	$I_{row4} = 4.8\ I_m$	$4V_m$	$19.2\ V_m\ I_m$
	$I_{row5} = 3.7\ I_m$	$5V_m$	$18.5\ V_m\ I_m$
DS	$I_{row1} = 5.0\ I_m$	V_m	$5.0\ V_m\ I_m$
	$I_{row2} = 5.0\ I_m$	$2V_m$	$10.0\ V_m\ I_m$
	$I_{row3} = 2.8\ I_m$	$3V_m$	$8.4\ V_m\ I_m$

	$I_{row4} = 5.0\ I_m$	$4V_m$	$20.0\ V_m\ I_m$
	$I_{row5} = 5.0\ I_m$	$5V_m$	$25.0\ V_m\ I_m$
LS	$I_{row1} = 2.8\ I_m$	V_m	$2.8\ V_m\ I_m$
	$I_{row2} = 5.0\ I_m$	$2V_m$	$10.0\ V_m\ I_m$
	$I_{row3} = 5.0\ I_m$	$3V_m$	$15.0\ V_m\ I_m$
	$I_{row4} = 5.0\ I_m$	$4V_m$	$20.0\ V_m\ I_m$
	$I_{row5} = 5.0\ I_m$	$5V_m$	$25.0\ V_m\ I_m$
OE	$I_{row1} = 4.3\ I_m$	V_m	$4.3\ V_m\ I_m$
	$I_{row2} = 4.8\ I_m$	$2V_m$	$9.6\ V_m\ I_m$
	$I_{row3} = 5.0\ I_m$	$3V_m$	$15.0\ V_m\ I_m$
	$I_{row4} = 4.3\ I_m$	$4V_m$	$17.2\ V_m\ I_m$
	$I_{row5} = 4.4\ I_m$	$5V_m$	$22.0\ V_m\ I_m$
Skyscraper	$I_{row1} = 3.9\ I_m$	V_m	$3.9\ V_m\ I_m$
	$I_{row2} = 5.0\ I_m$	$2V_m$	$10.0\ V_m\ I_m$
	$I_{row3} = 4.1\ I_m$	$3V_m$	$12.3\ V_m\ I_m$
	$I_{row4} = 4.8\ I_m$	$4V_m$	$19.2\ V_m\ I_m$
	$I_{row5} = 5.0\ I_m$	$5V_m$	$25.0\ V_m\ I_m$
CS	$I_{row1} = 4.3\ I_m$	V_m	$4.3\ V_m\ I_m$
	$I_{row2} = 4.3\ I_m$	$2V_m$	$8.6\ V_m\ I_m$
	$I_{row3} = 4.8\ I_m$	$3V_m$	$14.4\ V_m\ I_m$
	$I_{row4} = 4.8\ I_m$	$4V_m$	$19.2\ V_m\ I_m$
	$I_{row5} = 4.6\ I_m$	$5V_m$	$23.0\ V_m\ I_m$
SuDoKu	$I_{row1} = 4.1\ I_m$	V_m	$4.1\ V_m\ I_m$
	$I_{row2} = 4.6\ I_m$	$2V_m$	$9.2\ V_m\ I_m$
	$I_{row3} = 5.0\ I_m$	$3V_m$	$15.0\ V_m\ I_m$

	$I_{row4} = 5.0\ I_m$	$4V_m$	$20.0\ V_m\ I_m$
	$I_{row5} = 4.1\ I_m$	$5V_m$	$20.5\ V_m\ I_m$
MS	$I_{row1} = 4.3\ I_m$	V_m	$4.3\ V_m\ I_m$
	$I_{row2} = 4.8\ I_m$	$2V_m$	$9.6\ V_m\ I_m$
	$I_{row3} = 4.8\ I_m$	$3V_m$	$14.4\ V_m\ I_m$
	$I_{row4} = 4.6\ I_m$	$4V_m$	$18.4\ V_m\ I_m$
	$I_{row5} = 4.3\ I_m$	$5V_m$	$21.5\ V_m\ I_m$

Table 5.6 provides data regarding simulated values of I, V and P of distinct configurations at SN condition. The performance of SuDoKu and magic square is superior than other topologies. The highest value of power achieved is 2760 W.

For SN case, the GMPP comes out to be narrow. Notably, rest of the method flames out with respect to MS with a little difference in power. This is because MS acquires different arrangement of modules as compared to other topologies.

Table 5.6 Configurations Data Under SN Pattern

Configurations	**I(Amp.)**	**V(Volt)**	**P(Watt)**
SP	20.69	112.37	2324
TCT	22.98	114.90	2641
BL	22.11	114.10	2523
HC	21.86	113.45	2480
LD	21.20	112.74	2390
PRM-FEC	23.32	116.60	2719
Futoshiki	23.10	116.90	2700
DS	22.64	116.76	2643
LS	22.72	117.48	2669
OE	22.85	116.42	2660
Skyscraper	22.42	117.91	2644

CS	23.33	117.10	2732
SuDoKu	23.49	117.50	2760
MS	23.49	117.50	2760

The table 5.7 shows that in SW case, MS achieved highest power of 2550 W with reference to other configurations.

The same process is repeated as in SN scenario and their powers are evaluated and compared. The shadowing pattern and variations in irradiances are dispersed well via SuDoKu and MS methods with respect to rest of the configurations.

Table 5.7 Configurations Data Under SW Pattern

Configurations	**I(Amp.)**	**V(Volt)**	**P(Watt)**
SP	18.67	98.13	1832
TCT	20.12	100.60	2025
BL	19.83	99.21	1967
HC	19.94	99.10	1976
LD	19.74	98.89	1952
PRM-FEC	21.22	106.10	2251
Futoshiki	21.69	106.80	2316
DS	20.58	105.42	2170
LS	21.51	110.20	2370
OE	21.80	110.61	2411
Skyscraper	21.19	111.82	2369
CS	21.25	108.36	2303
SuDoKu	21.51	110.20	2370
MS	22.58	112.90	2550

The table 5.8 provides comparison among simulated values of all topologies in LN case. It is found that MS method attains highest power among all.

As only 2 columns get distinct irradiance, there is a little difference between MS and rest of the topologies. Consequently, MS method has the capability to disperse shade more effectively even at LN shading scenario.

Table 5.8 Configurations Data Under LN pattern

Configurations	I(Amp.)	V(Volt)	P(Watt)
SP	20.76	112.84	2343
TCT	22.96	114.80	2636
BL	21.10	112.43	2372
HC	20.81	113.64	2365
LD	21.10	112.43	2372
PRM-FEC	23.42	117.10	2743
Futoshiki	23.10	118.50	2737
DS	22.64	117.30	2656
LS	22.90	118.10	2704
OE	23.50	117.30	2757
Skyscraper	23.15	117.85	2728
CS	22.70	117.60	2666
SuDoKu	23.44	117.20	2747
MS	23.99	119.90	2877

The data obtained by implementing LW shading scenario is represented by table 5.9. It is seen MS provides greatest power of 1719 W among rest of the configurations.

Table 5.9 Configurations Data Under LW pattern

Configurations	I(Amp.)	V(Volt)	P(Watt)
SP	16.49	91.38	1507
TCT	17.93	89.63	1607
BL	17.70	89.68	1587
HC	17.81	89.37	1592
LD	17.54	90.32	1584

PRM-FEC	17.95	89.72	1612
Futoshiki	18.20	90.73	1651
DS	17.90	91.10	1630
LS	18.38	91.62	1684
OE	18.27	91.54	1672
Skyscraper	18.15	90.69	1646
CS	18.38	91.62	1684
SuDoKu	18.24	91.21	1644
MS	18.54	92.72	1719

Table 5.10 Configurations Data Under Diagonal pattern

Configurations	**I(Amp.)**	**V(Volt)**	**P(Watt)**
SP	20.29	100.64	2042
TCT	23.50	117.50	2761
BL	22.71	116.50	2646
HC	22.14	116.20	2573
LD	22.20	112.90	2507
PRM-FEC	21.82	111.50	2433
Futoshiki	21.52	113.30	2438
DS	21.18	115.61	2449
LS	21.97	114.38	2513
OE	22.81	112.34	2562
Skyscraper	21.53	115.91	2496
CS	22.16	114.80	2544
SuDoKu	22.46	112.30	2522
MS	23.50	117.50	2761

The simulated data is evaluated and presented in table 5.10 for diagonal shading case. In this, TCT and MS occupies same position having power of 2761W which is highest among all topologies.

The parameters such as P, V and I of various topologies given in figures 5.16-5.18. MS method gives maximum power at all shading cases. In MS, mostly modules work actively as shadow gets dispersed in uneven pattern. Thus, MS attain greatest output power and highest efficiency with respect to other configurations. Table 5.11 shows total power of MS which enhances with reference to other configurations.

Table 5.11 Percentage increase in MS power

Shading Patterns	SP (%)	TCT (%)	BL (%)	HC (%)	LD (%)	PRM-FEC (%)	Futoshiki (%)	DS (%)	LS (%)	OE (%)	Skyscraper (%)	CS (%)	SuDoKu (%)
SN	18.7	4.5	9.4	11.3	15.5	1.5	2.2	4.4	3.4	3.8	4.3	1.0	0
SW	39.1	25.9	29.6	29.0	30.6	13.3	10.1	17.5	7.6	5.8	7.6	10.7	7.6
LN	22.8	9.1	21.3	21.6	21.3	4.9	5.1	8.3	6.4	4.4	5.5	7.9	4.7
LW	14.0	7.0	8.3	8.0	8.5	6.6	4.1	5.5	2.0	2.8	4.4	2.0	3.3
Diagonal	35.2	0	4.3	7.3	10.1	13.5	13.2	12.7	9.9	7.8	10.6	8.5	9.5

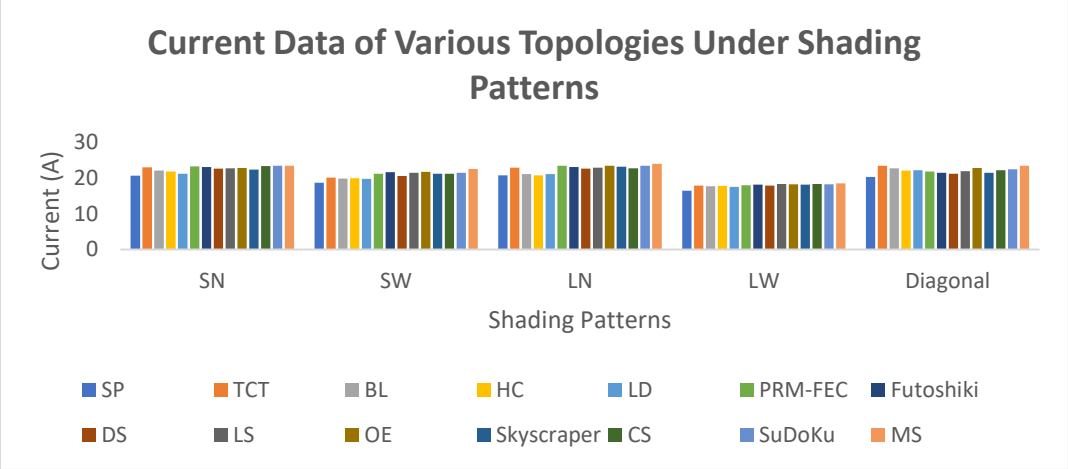

Figure 5.16 Current Data of Various Topologies Under Shading Patterns

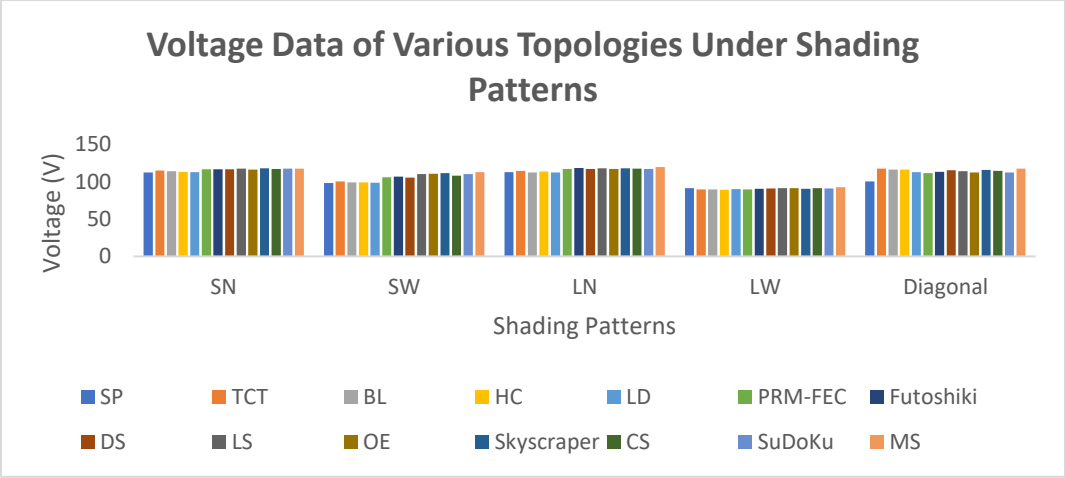

Figure 5.17 Voltage Data of Various Topologies Under Shading Patterns

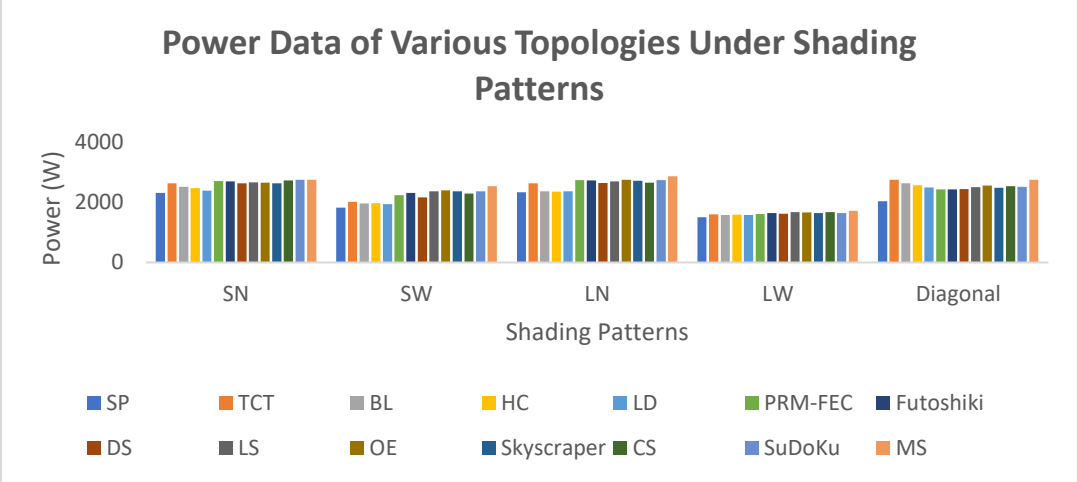

Figure 5.18 Power Data of Various Topologies Under Shading Patterns

The mismatch losses can be defined as the impact of PV modules interconnections which have different conditions. The expression of ML is described in equation 62.

Mismatch power loss = GMPPSTC – GMPPPPS (62)

The fill factor provides quality index of an array. The mathematical expression of it is given in equation 63.

FF = (Max. Power at PS)/(Rated power of PV array) (63)

The efficiency can be defined as the ratio of highest power to the product of irradiance and array area. Mathematically it is given in equation 64.

$$\text{Efficiency} = (\text{Max.Power})/(\text{Irradiation} * \text{Area of array}) \quad (64)$$

Table 5.12 provides the data regarding ML, FF and efficiency of distinct topologies at SN shading scenario. The largest efficiency is 9.66% which is acheived for SuDoKu and MS.

Table 5.12 Comparing Performance Data Under SN pattern

Configurations	ML (W)	FF	Efficiency(%)
SP	1325	0.389	8.13
TCT	1008	0.442	9.24
BL	1126	0.422	8.80
HC	1169	0.415	8.59
LD	1259	0.400	8.36
PRM-FEC	930	0.455	9.51
Futoshiki	949	0.452	9.45
DS	1006	0.442	9.25
LS	980	0.447	9.34
OE	989	0.445	9.31
Skyscraper	1005	0.443	9.25
CS	917	0.457	9.56
SuDoKu	889	0.462	9.66
MS	889	0.462	9.66

The various topologies at SW shade is shown by table 5.13 in which the maximum efficiency of 9.55%. is achieved by MS method.

Table 5.13 Comparing Performance Data Under SW pattern

Configurations	ML (W)	FF	Efficiency(%)
SP	1817	0.307	7.23
TCT	1624	0.339	8.00
BL	1682	0.329	7.77
HC	1673	0.331	7.80
LD	1697	0.327	7.71
PRM-FEC	1398	0.376	8.89
Futoshiki	1333	0.388	9.00
DS	1479	0.363	8.57
LS	1279	0.397	9.36
OE	1238	0.404	9.48
Skyscraper	1280	0.397	9.35
CS	1346	0.386	9.09
SuDoKu	1279	0.396	9.36
MS	1099	0.426	9.55

As per various parameters, it has been evaluated that MS method at LN shade obtain maximum efficiency of 10.24% as given table 5.14.

Table 5.14 Comparing Performance Data Under LN pattern

Configurations	ML (W)	FF	Efficiency(%)
SP	1306	0.392	8.34
TCT	1013	0.441	9.39
BL	1227	0.397	8.45
HC	1284	0.396	8.42
LD	1277	0.397	8.45
PRM-FEC	906	0.459	9.77
Futoshiki	912	0.458	9.75
DS	993	0.445	9.46

LS	945	0.453	9.63
OE	892	0.462	9.82
Skyscraper	921	0.457	9.71
CS	983	0.446	9.49
SuDoKu	902	0.460	9.78
MS	772	0.481	10.24

The MS topology at LW shade provides greatest efficiency of 8.26% while rest of the topologies provides efficiencies as shown by table 5.15.

Table 5.15 Comparing Performance Data Under LW pattern

Configurations	**ML (W)**	**FF**	**Efficiency(%)**
SP	2142	0.252	7.24
TCT	2042	0.269	7.72
BL	2062	0.266	7.63
HC	2057	0.267	7.65
LD	2065	0.265	7.61
PRM-FEC	2037	0.270	7.75
Futoshiki	1998	0.276	7.93
DS	2019	0.273	7.83
LS	1965	0.282	8.09
OE	1977	0.280	8.03
Skyscraper	2003	0.276	7.91
CS	1965	0.282	8.09
SuDoKu	1985	0.278	8.00
MS	1930	0.287	8.26

Table 5.16 gives data regarding various topologies at diagonal shading scenario. The maximum efficiency is 9.41% which is achieved for TCT and MS topologies.

Table 5.16 Comparing Performance Data Under Diagonal pattern

Configurations	ML (W)	FF	Efficiency(%)
SP	1607	0.342	6.96
TCT	888	0.462	9.41
BL	1003	0.443	9.02
HC	1076	0.431	8.77
LD	1142	0.420	8.54
PRM-FEC	1216	0.407	8.30
Futoshiki	1211	0.408	8.31
DS	1200	0.410	8.35
LS	1136	0.421	8.56
OE	1087	0.429	8.73
Skyscraper	1153	0.418	8.51
CS	1105	0.426	8.67
SuDoKu	1127	0.422	8.60
MS	888	0.462	9.41

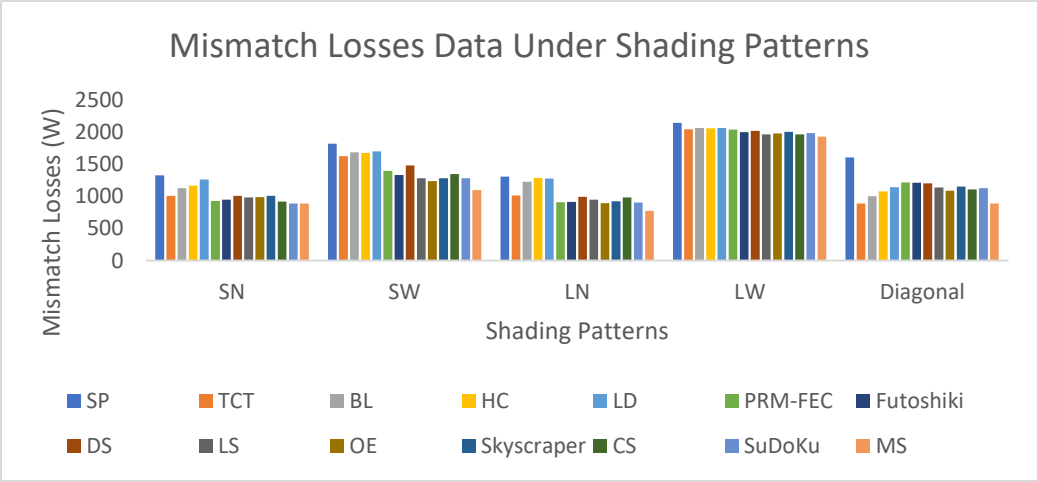

Figure 5.19 Mismatch Losses Data Under Shading Patterns

The figures 5.19-5.21 represents various topologies comparison based on parameters - ML, FF and efficiency. MS method extracts highest efficiency under all shading cases.

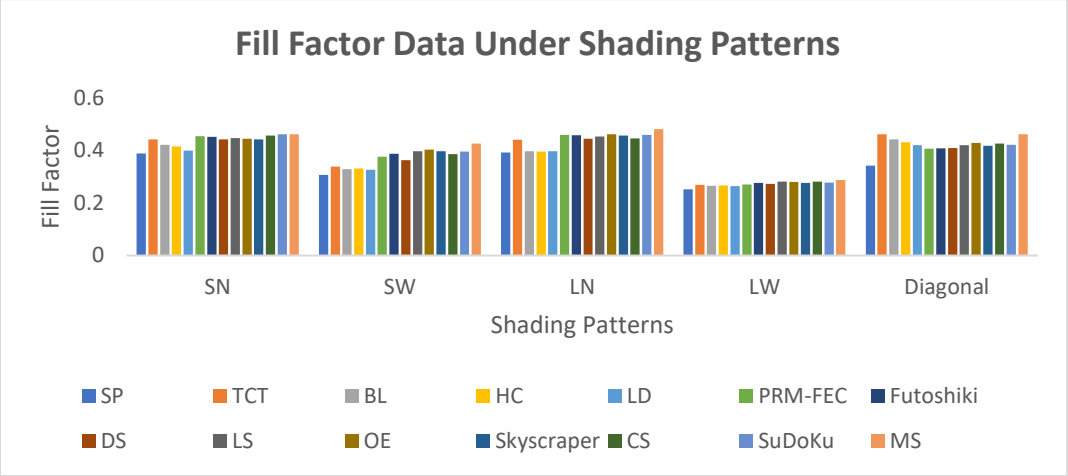

Figure 5.20 Fill Factor Data Under Shading Patterns

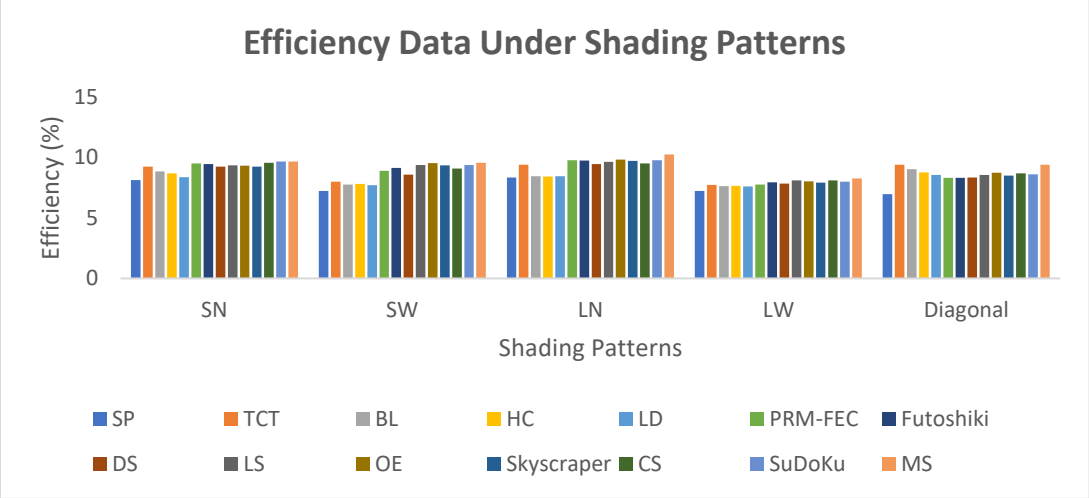

Figure 5.21 Efficiency Data Under Shading Patterns

CHAPTER 6

CONCLUSION AND FUTURE SCOPE

6.1 Conclusion

Though gaining wide scale popularity from small scale stand-alone to larger grid-tied applications, the PV industry faces a big challenge of maximizing the efficiency and minimizing the cost of energy generation. This thesis studies the effects of shading patterns on random cells within a module of solar cells. The main contributions of this work are:

a) Simple and accurate models of solar cells at distinct shading patterns that are modeled in MATLAB and the data have been compared.

b) Reconfigured methods are implemented to improve the functioning of system at the specified patterns.

c) The use of bypass diodes as a preventive measure to counter the reverse bias operation of solar cells due to effects of shading has been modeled.

The functioning of 5 × 5 PV array depends on fourteen topologies are studied and evaluated comprehensively via MATLAB/SIMULINK. The features that are included for measuring the working are I, V, P, ML, FF and efficiency. Table 5.1 presents SuDoKu and MS are superior with power of 2760 W than other topologies under SN pattern. The magic square technique obtained maximum output power of 2550 W, 2877 W and 1719 W under SW, LN and LW pattern respectively as shown in Table 5.2 to Table 5.4. TCT data matches with MS along with highest power of 2761 W for diagonal shade as indicated in Table 5.5. It is visible in table 5.6 that magic square power increases maximum of 25.9 % with reference to TCT under SW scenario. The power losses are greatest in TCT connection i.e., 1008 W under SN scenario as given in Table 5.7. Table 5.10 shows that losses of TCT is 2042 W which is greatest in all the configurations at LW shade. Table 5.9 shows that magic square has obtained the maximum efficiency of 10.24 % with respect to other configurations at LN shading condition. TCT has minimum efficiency of 7.72 % with reference to rest of the topologies at LW scenario as seen in table 5.10. The FF also changes

with various shading scenarios. FF is minimum at LW shade i.e., 0.269 and maximum in LN shade i.e., 0.481. The efficiencies may be distinct for every topology at various shading scenarios but by evaluating this work, magic square technique is superior and have largest efficiency at all shading conditions.

The concept of Magic Square technique has contributed a lot towards the society by performing good under shading scenarios. As the demand for electricity is increasing day by day, so world is moving towards renewable energy and reducing its dependence on coal, gas and fuels. Solar energy is widely adapted in providing electricity but shading due to dust, high rise buildings, trees, moving clouds etc. limits its efficiency. So, Magic Square method is adopted in this work which provides best efficiency among all topologies and contribute in fulfillment of electricity demands.

6.2 Future Scope

The major objective of this thesis is to investigate into the impact of shade on output of the PV system and the overall efficiency of the PV system. In this context some important design and control aspects along with the configurations that help in enhancing power of PV system are presented. However, still there are some areas which can be explored in continuation of this work. Some suggestions for further investigations in this field are as follows.

The work has mainly concentrated on the PV system, where crystalline-silicon PV panels are considered for the study. The study could be extended to thin film technology based solar cells. The thin film technology is promising due to its lower cost but is less efficient. Hence, thin film a-Si based system requires more space and modules as compared to c-Si modules based PV system for the same output power. It may be interesting to explore the various options of improving the output power at reasonable cost for such systems.

The work has not considered any type of optimization objective function in the evaluation of the various alternatives suggested. It may be interesting to devise the multi-objective function that simultaneously includes the cost minimization, power maximization, maximization of the inverter utilization factors etc.

REFERENCES

1. S. R. Chowdhury, H. Saha, "Maximum power point tracking of partially shaded solar photovoltaic arrays," Solar Energy Materials and Solar Cells, vol. 94, pp. 1441–1447, 2010.
2. F. M. Moreno, J. Munoz, E. Lorenzo, "Experimental model to estimate shading losses on PV arrays," Solar Energy Materials & Solar Cells, vol. 94, pp. 2298–2303, 2010.
3. Y. J. Wang, P. C. Hsu, "Analytical modelling of partial shading and different orientation of photovoltaic modules," IET Renewable Power Generation, vol. 4, issue 3, pp. 272–282, 2010.
4. E. D. Dorado, A. S. Garcia, C. Carrillo, J. Cidras, "Influence of the shadows in photovoltaic systems with different configurations of bypass diodes," in Proc. IEEE International Symposium on Power Electronics, Electrical Drives, Automation and Motion, pp. 134-139, 2010.
5. S. Moballegh, J. Jiang, "Partial shading modeling of photovoltaic system with experimental validations," in Proc. IEEE Conference on Power and Energy Society General Meeting, pp. 1-9, 2011.
6. M. Z. S. El-Dein, M. Kazerani, M. M. A. Salama, "Novel configurations for photovoltaic farms to reduce partial shading losses," in Proc. IEEE Conference on Power and Energy Society General Meeting, pp. 1-5, 2011.
7. K. Ishaque, Z. Salam, Syafaruddin, "A comprehensive MATLAB/Simulink PV system simulator with partial shading capability based on two diode model," Solar Energy, vol. 85, pp. 2217–2227, 2011.
8. A. Maki, S. Valkealahti, J. Leppaaho, "Operation of series connected silicon based photovoltaic modules under partial shading conditions," Progress in Photovoltaics: Research and Applications, vol. 20, pp. 298–309, 2012.
9. R. Kadri, H. Andrei, J. P. Gaubert, T. Ivanovici, G. Champenois, P. Andrei, "Modeling of the photovoltaic cell circuit parameters for optimum connection model and real time emulator with partial shadow conditions," Energy, vol. 42, pp. 57-67, 2012.
10. K. Ding, X. G. Bian, H. H. Liu, T. Peng, "A MATLAB/Simulink based PV module model and its application under conditions of non-uniform irradiance," IEEE Transactions on Energy Conversion, vol. 27, issue 4, pp. 864-872, 2012.

11. A. Maki, S. Valkealahti, "Power losses in long string and parallel connected short strings of series-connected silicon-based photovoltaic modules due to partial shading conditions," IEEE Transactions on Energy Conversion, vol. 27, issue 1, pp.173-183, 2012.

12. R. Ramaprabha, B. L. Mathur, "A comprehensive review and analysis of solar photovoltaic array configurations under partial shaded conditions," International Journal of Photo-energy, vol. 2012, pp. 1-16, 2012.

13. Y. J. Wang, and S. S. Lin, "Analysis of a partially shaded PV array considering different module connection schemes and effects of bypass diodes," in Proc. IEEE Conference on Utility Exhibition on Power and Energy Systems: Issues and Prospects for Asia, pp. 1-7, 2012.

14. L. F. L. Villa, D. Picault, B. Raison, S. Bacha, A. Labonne, "Maximizing the power output of partially shaded photovoltaic plants through optimization of the interconnections among its modules," IEEE Journal of Photovoltaics, vol. 2, issue 2, pp. 154-163, 2012.

15. L. Cristaldi, M. Faifer, M. Rossi, and F. Ponci, ''A simple photovoltaic panel model: Characterization procedure and evaluation of the role of environmental measurements,'' IEEE Trans. Instrum. Meas., vol. 61, issue 10, pp. 2632–2641, 2012.

16. F. Lu, S. Guo, T. M. Walsh, A. G. Aberle, "Improved PV module performance under partial shading conditions," Energy Procedia, vol. 33, pp. 248 – 255, 2013.

17. M. Seyedmahmoudian, S. Mekhilef, R. Rahmani, R. Yusof, E. T. Renani, "Analytical modeling of partially shaded photovoltaic systems," Energies, vol. 6, pp. 128- 144, 2013.

18. H. Tian, F. M. David, K. Ellis, E. Muljadi, P. Jenkins, "Determination of the optimal configuration for a photovoltaic array depending on the shading condition," Solar Energy, vol. 95, pp. 1–12, 2013.

19. T. H. Jung, J. W. Ko, G. H. Kang, H. K. Ahn, "Output characteristics of PV module considering partially reverse biased conditions," Solar Energy, vol. 92, pp. 214–220, 2013.

20. C. A. Ramoz-Paza, J. D. Bastidas, A. J. SaavendraMontes, "Experimental validation of a model for photovoltaic arrays in total cross-tied configuration," Dyna, vol. 80, pp. 191-199, 2013.

21. E. D. Dorado, J. Cidra, C. Carrillo, "Discrete I–V model for partially shaded PV arrays," Solar Energy, vol. 103, pp. 96–107, 2014.

22. L. Fialho, R. Melicio, V.M.F. Mendes, J. Figueiredo, M. C. Pereira, "Effect of shading on series solar modules: simulation and experimental results," Procedia Technology, vol. 17, pp. 295 – 302, 2014.

23. T. Ma, H. Yang, L. Lu, "Development of a model to simulate the performance characteristics of crystalline silicon photovoltaic modules/strings/arrays," Solar Energy, vol. 100, pp. 31–41, 2014.

24. S. Vijayalekshmy, S. R. Iyer, B. Beevi, "Comparative analysis on the performance of a short string of series connected and parallel connected photovoltaic array under partial shading," Journal of Institution Engineers India- Series B, vol. 96, issue 3, pp. 217-226, 2014.

25. S. Moballegh, J. Jiang, "Modeling, prediction, and experimental validations of power peaks of PV arrays under partial shading conditions," IEEE Transactions on Sustainable Energy, vol. 5, issue 1, pp. 293-300, 2014.

26. F. Belhachat, C. Larbes, "Modeling, analysis and comparison of solar photovoltaic array configurations under partial shading conditions," Solar Energy, vol. 120, pp. 399–418, 2015.

27. S. Malathy, R. Ramaprabha, "Comprehensive analysis on the role of array size and configuration on energy yield of photovoltaic systems under shaded conditions," Renewable and Sustainable Energy Reviews, vol. 49, pp. 672-679, 2015.

28. L. A. T. Grisales, C. A. R. Paja, Y. A. J. S. Montes, "Equivalent circuits for simulating irregular PV arrays under partial shading conditions," Technologicas, vol. 18, issue 35, pp. 57-69, 2015.

29. P. Vengatesh and S. E. Rajan, ''Investigation of the effects of homogeneous and heterogeneous solar irradiations on multicrystal PV module under various configurations,'' IET Renew. Power Gener., vol. 9, issue 3, pp. 245–254, 2015.

30. P. D. S. Vicente, T. C. Pimenta, E. R. Ribeiro, "Photovoltaic array reconfiguration strategy for maximization of energy production," International Journal of Photo Energy, pp. 2-11, 2015.

31. M. L. Gutierrez-Orozco, G. Spagnuolo, J. M. Scarpetta-Ramirez, G. Petrone, and C. A. Ramos-Paja, ''Optimized configuration of mismatched photovoltaic arrays,'' IEEE J. Photovolt., vol. 6, issue 5, pp. 1210–1220, 2016.

32. H. Braun, S. T. Buddha, V. Krishnan, C. Tepedelenlioglu, A. Spanias, M. Banavar, D. Srinivasan, "Topology reconfiguration for optimization of photovoltaic array output," Sustainable Energy, Grids and Networks, vol. 6, pp. 58–69, 2016.

33. H. S. Sahu, S. K. Nayak, and S. Mishra, ''Maximizing the power generation of a partially shaded PV array,'' IEEE J. Emerg. Sel. Topics Power Electron., vol. 4, issue 2, pp. 626–637, Jun. 2016.

34. S. Mohammadnejad, A. Khalafi, S. M. Ahmadi, "Mathematical analysis of total cross-tied photovoltaic array under partial shading condition and its comparison with other configurations," Solar Energy, vol. 133, 501– 511, 2016.

35. A. S. Yadav, R. K. Pachauri, Y. K. Chauhan, "Comprehensive investigation of PV arrays with puzzle shade dispersion for improved performance," Solar Energy, vol. 129, pp. 256–285, 2016.

36. R. Ahmad, A. F. Murtaza, H. A. Sher, U. T. Shami, S. Olalekan, "An analytical approach to study partial shading effects on PV array supported by literature," Renewable and Sustainable Energy Reviews, vol. 74, pp. 721-732, 2017.

37. A. Mehiri, A.-K. Hamid, and S. Almazrouei, ''The effect of shading with different PV array configurations on the grid-connected PV system,'' in Proc. Int. Renew. Sustain. Energy Conf. (IRSEC), Tangier, Morocco, pp. 1–6, 2017.

38. A. S. Yadav, R. K. Pachauri, Y. K. Chauhan, S. Choudhury, and R. Singh, ''Performance enhancement of partially shaded PV array using novel shade dispersion effect on magic-square puzzle configuration,'' Sol. Energy, vol. 144, pp. 780–797, 2017.

39. R. P. Vengatesh, and S. E. Rajan, "Analysis of PV module connected in different configurations under uniform and non-uniform solar radiations," International Journal of Green Energy, vol. 14, issue 13, pp. 1507-1516, 2017.

40. X. Qing, H. Sun, X. Feng, and C. Y. Chung, ''Submodule-based modeling and simulation of a series-parallel photovoltaic array under mismatch conditions,'' IEEE J. Photovolt., vol. 7, issue 6, pp. 1731–1739, 2017.

41. S. Bana, and R. P. Saini, "Experimental investigation on power output of different photovoltaic array configurations under uniform and partial shading scenarios," Energy, vol. 127, pp. 438-453, 2017.

42. N. Belhaouas, M. S. A. Cheikh, P. Agathoklis, M. R. Oularbi, B. Amrouche, K. Sedraoui, N. Djilali, "PV array power output maximization under partial shading using new shifted PV array arrangements," Applied Energy, vol. 187, pp. 326–337, 2017.

43. M. J. Bosco, and M. C. Mabel, "A novel cross diagonal view configuration of a PV system under partial shading condition," Solar Energy, vol. 158, pp. 760-773, 2017.

44. S. C. Pareek, and R. Dahiya, "Optimal interconnections o address partial shading losses in solar photovoltaic arrays," Solar Energy, vol. 155, pp. 537-551, 2017.

45. P. R. Satpathy, R. Sharma, S. Jena, "A shade dispersion interconnection scheme for partially shaded modules in a solar PV array network," Energy, vol. 139, pp. 350- 365, 2017.

46. O. Khan, W. Xiao, and M. S. E. Moursi, ''A new PV system configuration based on submodule integrated converters,'' IEEE Trans. Power Electron., vol. 32, issue 5, pp. 3278–3284, 2017.

47. Y. Mochizuki and T. Yachi, ''Relationship between power generated and series/parallel solar panel configurations for 3D fibonacci PV modules,'' in Proc. IEEE 6th Int. Conf. Renew. Energy Res. Appl. (ICRERA), San Diego, CA, USA, pp. 126–130, 2017.

48. Y. Mochizuki and T. Yachi, ''Effective series-parallel cell configuration in solar panels for FPM power generation forest,'' in Proc. 7th Int. Conf. Renew. Energy Res. Appl. (ICRERA), Paris, France, pp. 294–300, 2018.

49. M. Orkisz, ''Estimating effects of individual PV panel failures on PV array output,'' IEEE Trans. Ind. Appl., vol. 54, issue 5, pp. 4825–4832, 2018.

50. F. Iraji, E. Farjah, and T. Ghanbari, ''Optimisation method to find the best switch set topology for reconfiguration of Photovoltaic panels,'' IET Renew. Power Gener., vol. 12, issue 3, pp. 374–379, 2018.

51. B. Veerasamy, T. Takeshita, A. Jote, and T. Mekonnen, ''Mismatch loss analysis of PV array configurations under partial shading conditions,'' in Proc. 7th Int. Conf. Renew. Energy Res. Appl. (ICRERA), Paris, France, pp. 1162–1167, 2018.

52. Huagen Xiao, Xiaoyu Yi, Shiqi Ding, Shi Su, "Optimal configuration method based on optimal expected power characteristics for micro power supply and energy storage device", IET Renewable Power Generation, vol. 12, issue 16, pp. 1876-1882, 2018.

53. J. D. B. Rodriguez, L. A. T. Grisales, D. G. Montoya, C. A. R. Paja, G. G. Spagnuolo, "General modeling procedure for photovoltaic arrays," Electric Power Systems Research, vol. 155, pp. 67-79, 2018.

54. Gurusamy Madhusudanan, Subramaniam Senthilkumar, I. Anand, and Padmanaban Sanjeevikumar, "A shade dispersion scheme using Latin square arrangement to enhance power production in solar photovoltaic array under partial shading conditions", Journal of Renewable and Sustainable Energy, vol. 10, pp. 1-14, 2018.

55. A. Xenophontos and A. M. Bazzi, ''Model-based maximum power curves of solar photovoltaic panels under partial shading conditions,'' IEEE J. Photovolt., vol. 8, issue 1, pp. 233–238, 2018.

56. L. E. Iysaouy, M. Lahbabi, and A. Oumnad, ''A novel magic square view topology of a pv system under partial shading condition,'' in Proc. Technol. Mater. Renew. Energy, Environ. Sustain. (TMREES), Athens, Greece, pp. 1182–1190, 2018.

57. B. Dhanalakshmi, N. Rajasekar, "A novel Competence Square based PV array reconfiguration technique for solar PV maximum power extraction", Energy Conversion and Management, vol. 174, pp. 897-912, 2018.

58. K. Lappalainen and S. Valkealahti, ''Fluctuation of PV array global maximum power point voltage during irradiance transitions caused by clouds,'' IET Renew. Power Gener., vol. 13, issue 15, pp. 2864–2870, 2019.

59. C. W. Hansen and B. H. King, ''Determining series resistance for equivalent circuit models of a PV module,'' IEEE J. Photovolt., vol. 9, issue 2, pp. 538–543, 2019.

60. L. Caetano, G. Caaixeta, T. Lima, J. Oliveira, R. Ramos, and A. Rodrigo, ''Modelling of a multipurpose photovoltaic generator block using ATP-EMTP,'' IEEE Latin Amer. Trans., vol. 17, issue 02, pp. 203–209, 2019.

61. R. Pachauri, R. Singh, A. Gehlot, R. Samakaria, S. Choudhury, "Experimental analysis to extract maximum power from PV array reconfiguration under partial shading conditions", Engineering Science and Technology, an International Journal, vol. 22, pp. 109– 130, 2019.

62. G. S. Krishna, T. Moger, "Improved Su-Do-Ku reconfiguration technique for total-cross-tied PV array to enhance maximum power under partial shading conditions", Renewable and Sustainable Energy Reviews, vol. 109, pp. 333–348, 2019.

63. I. Nasiruddin, S. Khatoon, M. F. Jalil, R.C. Bansal, "Shade diffusion of partial shaded PV array by using odd-even structure", Solar Energy, vol. 181, pp. 519–529, 2019.

64. Vandana Jha, Uday Shankar Triar, "A detailed comparative analysis of different photovoltaic array configurations under partial shading conditions", Int Trans Electr Energ Syst., pp. 1-36, 2019.

65. M. S. S. Nihanth, J. P. Ram, D. S. Pillai, A. M.Y.M. Ghias, A. Garg, N. Rajasekar, "Enhanced power production in PV arrays using a new skyscraper puzzle based one-time reconfiguration procedure under partial shade conditions (PSCs)", Solar Energy, vol. 194, pp. 209–224, 2019.

66. Chayut Tubniyom, Rongrit Chatthaworn, Amnart Suksri, and Tanakorn Wongwuttanasatian, "Minimization of Losses in Solar Photovoltaic Modules by Reconfiguration under Various Patterns of Partial Shading", Energies, vol. 12, pp. 1-15, 2019.

67. H. N. Suresh and S. Rajanna, ''Performance enhancement of hybrid interconnected solar photovoltaic array using shade dispersion magic square puzzle pattern technique under partial shading conditions,'' Sol. Energy, vol. 194, pp. 602–617, 2019.

68. G. S. Krishna and T. Moger, "Reconfiguration strategies for reducing partial shading effects in photovoltaic arrays: State of the art," Solar Energy, vol. 182, pp. 429 – 452, 2019.

69. S. G. Krishna and T. Moger, ''Optimal SuDoKu reconfiguration technique for total-cross-tied PV array to increase power output under non-uniform irradiance,'' IEEE Trans. Energy Convers., vol. 34, issue 4, pp. 1973–1984, 2019.

70. K. Rajani and T. Kandipati, ''Maximum power enhancement under partial shadings using modified SuDoKu reconfiguration,'' CSEE J. Power Energy Syst., early access, 2020.

71. V. S. Bhadoria, R. K. Pachauri, S. Tiwari, S. P. Jaiswal, and H. H. Alhelou, ''Investigation of different BPD placement topologies for shaded modules in a series-parallel configured PV array,'' IEEE Access, vol. 8, pp. 216911–216921, 2020.

72. M. Premkumar, U. Subramaniam, T. S. Babu, R. M. Elavarasan, and L. Mihet-Popa, ''Evaluation of mathematical model to characterize the performance of conventional and hybrid PV array topologies under static and dynamic shading patterns,'' Energies, vol. 13, issue 12, pp. 1–37, 2020.

73. A. Ul-Haq, R. Alammari, A. Iqbal, M. Jalal, and S. Gul, ‘‘Computation of power extraction from photovoltaic arrays under various fault conditions,’’ IEEE Access, vol. 8, pp. 47619–47639, 2020.

74. D. Yousri, S. Mirjalili, S. B. Thanikanti, R. Natarajan, and M. Elsayed Abd Elaziz, “A novel objective function with artificial ecosystem-based optimization for relieving the mismatching power loss of large-scale photovoltaic array,” Energy Conversion and Management, vol. 225, issue 9, 2020.

75. G. Sagar, D. Pathak, P. Gaur, V. Jain, “A Su Do Ku puzzle based shade dispersion for maximum power enhancement of partially shaded hybrid bridge-linktotal-cross-tied PV array,” Solar Energy, vol. 204, pp. 161–180, 2020.

76. S. R. Pendem, S. Mikkili, and P. K. Bonthagorla, ‘‘PV distributed-MPP tracking: Total-cross-tied configuration of string-integrated-converters to extract the maximum power under various PSCs,’’ IEEE Syst. J., vol. 14, issue 1, pp. 1046–1057, 2020.

77. Aidha Muhammad Ajmala, Thanikanti Sudhakar Babua, Vigna K. Ramachandaramurthya, Dalia. Yousrib, Janaka B. Ekanayake, “Static and dynamic reconfiguration approaches for mitigation of partial shading influence in photovoltaic arrays”, Sustainable Energy Technologies and Assessments, vol. 40, pp. 1-23, 2020.

78. Zhen Zhu, Meiyi Hou, Lei Ding, Guofang Zhu, Zhaoyang Jin, “Optimal Photovoltaic Array Dynamic Reconfiguration Strategy Based on Direct Power Evaluation”, IEEE Access, Vol. 8, pp. 210267-210276, 2020.

79. Mayank Kumar, “Enhanced Solar PV Power Generation Under PSCs Using Shade Dispersion”, IEEE Transactions on Electron Devices, pp. 1-8, 2020.

80. Vishnu P. Madhanmohan, Abdul Saleem, and M. Nandakumar, “An Algorithm for Enhanced Performance of Photovoltaic Array Under Partial Shading Condition”, IEEE Access, vol. 8, pp. 176947 – 176959, 2020.

81. Praveen Kumar Bonthagorla, Suresh Mikkili, “Impact of Partial Shading on Various PV Array Configurations and Different Modeling Approaches for Harvesting Maximum Power from Shaded Modules by Reducing the Number of Cross-Ties”, IEEE Journal of Emerging and Selected Topics in Power Electronics, vol. 9, issue 2, 2021.

82. Mohammad Nor Rafiq Nazer; Abdulfattah Noorwali; Mohammad Faridun Naim Tajuddin; Mohammad Zubair Khan; Mohamad Afiq Izzat Ahmad Tazally, Jubaer Ahmed,

Thanikanti Sudhakar Babu, “Scenario-based Investigation on the Effect of Partial Shading Condition Patterns for Different Static Solar Photovoltaic Array Configurations”, IEEE Access, pp.1-22, 2021.

83. Rupendra Kumar Pachauri, Isha Kansal, Thanikanti Sudhakar Babu, Hassan Haes Alhelou, “Power Losses Reduction of Solar PV Systems Under Partial Shading Conditions Using Re-Allocation of PV Module-Fixed Electrical Connections”, IEEE Access, vol. 9, pp. 94789 - 94812, 2021.

84. D. Prince Winston, G. Karthikeyan, M. Pravin, O. Jeba Singh, A.G. Akash, S. Nithish, S. Kabilan, “Parallel power extraction technique for maximizing the output of solar PV array”, Solar Energy, vol. 213, pp. 102-117, 2021.

85. Smruti Madhura Maharana; Alivarani Mohapatra; Chidurala Saiprakash; Abhinaba Kundu, “Comparative analysis of different PV array configurations under partial shading conditions”, 3rd International Conference on Energy, Power and Environment: Towards Clean Energy Technologies, Shillong, Meghalaya, India, 2021.

86. Mohammed Alkahtani, Jiafeng Zhou, Yihua Hu, Fahad Alkasmoul, Zeryab Hassan Kiani, Colin Sokol Kuka, “An Experimental Investigation on Output Power Enhancement with Offline Reconfiguration for Non-Uniform Aging Photovoltaic Array to Maximize Economic Benefit”, IEEE Access, vol. 9, pp. 87510 – 87519, 2021.

87. H. Rezk, A. Fathy, and M. Aly, ‘‘A robust photovoltaic array reconfiguration strategy based on coyote optimization algorithm for enhancing the extracted power under partial shadow condition,’’ Energy Rep., vol. 7, pp. 109–124, 2021.

88. A. Srinivasan, S. Devakirubakaran; B. Meenakshi Sundaram; Praveen Kumar Balachandran; Santhan Kumar Cherukuri; D. Prince Winston; Thanikanti Sudhakar Babu; Hassan Haes Alhelou, “L-Shape Propagated Array Configuration With Dynamic Reconfiguration Algorithm for Enhancing Energy Conversion Rate of Partial Shaded Photovoltaic Systems”, IEEE Access, vol. 9, pp. 97661 – 97674, 2021.

89. Murugesan Palpandian, David Prince Winston, Balachandran Praveen Kumar, Cherukuri Santhan Kumar, Thanikanti Sudhakar Babu, Hassan Haes Alhelou, “A New Ken-Ken Puzzle Pattern Based Reconfiguration Technique for Maximum Power Extraction in Partial Shaded Solar PV Array”, IEEE Access, vol. 9, pp. 65824 – 65837, 2021.

90. Ali F Murtaza, Hadeed Ahmed Sher, Kamal Al-Haddad, Filippo Spertino, "Module Level Electronic Circuit based PV array for Identification and Reconfiguration of Bypass Modules", IEEE Transactions On Energy Conversion, 2021, Vol. 36, Issue: 1, pp. 380 – 389, 2021.

91. R. Pachauri, J. Bai, I. Kansal, O. Mahela, and B. Khan, "Shade dispersion methodologies for performance improvement of classical total-cross-tied photovoltaic array configuration under partial shading conditions," IET Renewable Power Generation, vol. 15, issue 2, 2021.

92. Chidurala Saiprakash; Alivarani Mohapatra; Byamakesh Nayak, "An A TT array configuration for performance enhancement of PV system under PSC", 1st International Conference on Power Electronics and Energy (ICPEE), Bhubaneswar, India, 2021.

93. Snigdha Sharma, Lokesh Varshney, Rajvikram Madurai Elavarasan, Akanksha Singh S. Vardhan, Aanchal Singh S. Vardhan, R. K. Saket, Umashankar Subramaniam and Eklas Hossain "Performance Enhancement of PV System Configurations Under Partial Shading Conditions Using MS Method", IEEE ACCESS, vol. 9, pp. 56630-56644, 2021.

94. R. Venkateswari, N. Rajasekar, "Power enhancement of PV system via physical array reconfiguration-based Lo Shu technique", Energy Cnversion and Management, vol. 215, pp. 1-22, 2021.

95. Snigdha Sharma, Lokesh Varshney, and R.K. Saket, "Comparative Evaluation of Novel Configurations Under Shading Conditions", Journal of Electrical Systems (JES), vol. 18, issue 1, pp. 97-108, 2022.